VOLUME 34 MARCH 1957 NUMBER 8

UNIVERSITY
OF MICHIGAN
MAR
ENGINEERING
LIBRARY

Canadian Journal of Technology

Editor: G. A. LEDINGHAM

Published by THE NATIONAL RESEARCH COUNCIL
OTTAWA CANADA

CANADIAN JOURNAL OF TECHNOLOGY

(*Formerly Section F, Canadian Journal of Research*)

Under the authority of the Chairman of the Committee of the Privy Council on Scientific and Industrial Research, the National Research Council issues THE CANADIAN JOURNAL OF TECHNOLOGY and six other journals devoted to the publication, in English or French, of the results of original scientific research. Matters of general policy concerning these journals are the responsibility of a joint Editorial Board consisting of: members representing the National Research Council of Canada; the Editors of the Journals; and members representing the Royal Society of Canada and four other scientific societies.

The Chemical Institute of Canada has chosen the Canadian Journal of Technology and the Canadian Journal of Chemistry as its medium of publication for scientific papers.

EDITORIAL BOARD

Representatives of the National Research Council

A. N. Campbell, *University of Manitoba*
G. E. Hall, *University of Western Ontario*
H. G. Thode, *McMaster University*
D. L. Thomson, *McGill University*
W. H. Watson (Chairman), *University of Toronto*

Editors of the Journals

D. L. Bailey, *University of Toronto*
T. W. M. Cameron, *Macdonald College*
H. E. Duckworth, *McMaster University*
G. A. Ledingham, *National Research Council*
Léo Marion, *National Research Council*
R. G. E. Murray, *University of Western Ontario*
K. A. C. Elliott, *Montreal Neurological Institute*

Representatives of Societies

D. L. Bailey, *University of Toronto*
Royal Society of Canada
T. W. M. Cameron, *Macdonald College*
Royal Society of Canada
H. E. Duckworth, *McMaster University*
Royal Society of Canada
Canadian Association of Physicists
K. A. C. Elliott, *Montreal Neurological Institute*
Canadian Physiological Society
R. G. E. Murray, *University of Western Ontario*
Canadian Society of Microbiologists
H. G. Thode, *McMaster University*
Chemical Institute of Canada
T. Thorvaldson, *University of Saskatchewan*, Royal Society of Canada

Ex officio

Léo Marion (Editor-in-Chief), *National Research Council*
F. T. Rosser, Director, Division of Administration, *National Research Council*

Manuscripts for publication should be submitted to Dr. Léo Marion, Editor-in-Chief, Canadian Journal of Technology, National Research Council, Ottawa 2, Canada.
(For instructions on preparation of copy, see **Notes to Contributors** (inside back cover).)

Proof, correspondence concerning proof, and orders for reprints should be sent to the Manager, Editorial Office (Research Journals), Division of Administration, National Research Council, Ottawa 2, Canada.

Subscriptions, renewals, requests for single or back numbers, and all remittances should be sent to Division of Administration, National Research Council, Ottawa 2, Canada. Remittances should be made payable to the Receiver General of Canada, credit National Research Council.

The journals published, frequency of publication, and prices are:

Canadian Journal of Biochemistry and Physiology	Monthly	$3.00 a year
Canadian Journal of Botany	Bimonthly	$4.00 a year
Canadian Journal of Chemistry	Monthly	$5.00 a year
Canadian Journal of Microbiology	Bimonthly	$3.00 a year
Canadian Journal of Physics	Monthly	$4.00 a year
Canadian Journal of Technology	Bimonthly	$3.00 a year
Canadian Journal of Zoology	Bimonthly	$3.00 a year

The price of single numbers of all journals is 75 cents.

Contents

Page

Determination of Sulphate Acid Ester in Unstabilized Cellulose Nitrate—*Paul E. Gagnon, Karl F. Keirstead, and Donald Yamasaki* - - - - - - - - - - - - - - - 477

The Design and Operation of a Cloud Chamber—*Louis A. Madonna* 485

Nickel–Cadmium Batteries. II. Impregnation of Positive Plates by Thermal Decomposition of Aqueous Nickel Nitrate—*P. L. Bourgault, Phyllis E. Lake, E. J. Casey, and A. R. Dubois* - - 495

Neutron Moisture Meter for Concrete—*J. Pawlik and J. W. T. Spinks* - - - - - - - - - - - - - - - - - 503

Vapor–Liquid Equilibrium Data for System: *n*-Octane–Propionic Acid, with Salt Effect—*A. I. Johnson, D. M. Ward, and W. F. Furter* - - - - - - - - - - - - - - - - - 514

Notes:

Microwave Refractometer Cavity Design—*Albert W. Adey* - - 519

Electrodeless Discharge Lamp Exciter—*D. S. Smith* - - - 521

A Note on Thermodynamic Consistency Tests of Binary Vapor–Liquid Equilibrium Data—*Benjamin C.-Y. Lu* - - - - - 523

Contents of Volume 34 - - - - - - - - - - - - - - 528

Printed in Canada *by* University of Toronto Press

CANADIAN JOURNAL OF TECHNOLOGY

Notes to Contributors

Manuscripts

(i) ***General.*** Manuscripts, in English or French, should be typewritten, double spaced, on paper 8½ × 11 in. **The original and one copy are to be submitted.** Tables and captions for the figures should be placed at the end of the manuscript. Every sheet of the manuscript should be numbered.

Style, arrangement, spelling, and abbreviations should conform to the usage of this journal. Names of all simple compounds, rather than their formulas, should be used in the text. Greek letters or unusual signs should be written plainly or explained by marginal notes. Superscripts and subscripts must be legible and carefully placed.

Manuscripts and illustrations should be carefully checked before they are submitted. Authors will be charged for unnecessary deviations from the usual format and for changes made in the proof that are considered excessive or unnecessary.

(ii) ***Abstract.*** An abstract of not more than about 200 words, indicating the scope of the work and the principal findings, is required, except in Notes.

(iii) ***References.*** References should be listed **alphabetically by authors' names,** numbered, and typed after the text. The form of the citations should be that used in this journal; in references to papers in periodicals, titles should not be given and only initial page numbers are required. The names of periodicals should be abbreviated in the form given in the most recent *List of Periodicals Abstracted by Chemical Abstracts.* All citations should be checked with the original articles and each one referred to in the text by the key number.

(iv) ***Tables.*** Tables should be numbered in roman numerals and each table referred to in the text. Titles should always be given but should be brief; column headings should be brief and descriptive matter in the tables confined to a minimum. Vertical rules should be used only when they are essential. Numerous small tables should be avoided.

Illustrations

(i) ***General.*** All figures (including each figure of the plates) should be numbered consecutively from 1 up, in arabic numerals, and each figure referred to in the text. The author's name, title of the paper, and figure number should be written in the lower left corner of the sheets on which the illustrations appear. Captions should not be written on the illustrations (see Manuscripts (i)).

(ii) ***Line Drawings.*** Drawings should be carefully made with India ink on white drawing paper, blue tracing linen, or co-ordinate paper ruled in blue only; any co-ordinate lines that are to appear in the reproduction should be ruled in black ink. Paper ruled in green, yellow, or red should not be used unless it is desired to have all the co-ordinate lines show. All lines should be of sufficient thickness to reproduce well. Decimal points, periods, and stippled dots should be solid black circles large enough to be reduced if necessary. Letters and numerals should be neatly made, preferably with a stencil (**do NOT use typewriting**) and be of such size that the smallest lettering will be not less than 1 mm. high when reproduced in a cut 3 in. wide.

Many drawings are made too large; originals should not be more than 2 or 3 times the size of the desired reproduction. In large drawings or groups of drawings the ratio of height to width should conform to that of a journal page but the height should be adjusted to make allowance for the caption.

The original drawings and one set of clear copies (e.g. small photographs) are to be submitted.

(iii) ***Photographs.*** Prints should be made on glossy paper, with strong contrasts. They should be trimmed so that essential features only are shown and mounted carefully, with rubber cement, on white cardboard with no space or only a **very** small space (less than 1 mm.) between them. In mounting, full use of the space available should be made (to reduce the number of cuts required) and the ratio of height to width should correspond to that of a journal page (4¾ × 7½ in.); however, allowance must be made for the captions. Photographs or groups of photographs should not be more than 2 or 3 times the size of the desired reproduction.

Photographs are to be submitted in duplicate; if they are to be reproduced in groups one set should be mounted, the duplicate set unmounted.

Reprints

A total of 50 reprints of each paper, without covers, are supplied free. Additional reprints, with or without covers, may be purchased.

Charges for reprints are based on the number of printed pages, which may be calculated approximately by multiplying by 0.6 the number of manuscript pages (double-spaced typewritten sheets, 8½ × 11 in.) and including the space occupied by illustrations. An additional charge is made for illustrations that appear as coated inserts. The cost per page is given on the reprint requisition which accompanies the galley.

Any reprints required in addition to those requested on the author's reprint requisition form must be ordered officially as soon as the paper has been accepted for publication.

Canadian Journal of Technology

Issued by THE NATIONAL RESEARCH COUNCIL OF CANADA

VOLUME 34 MARCH 1957 NUMBER 8

DETERMINATION OF SULPHATE ACID ESTER IN UNSTABILIZED CELLULOSE NITRATE[1]

By PAUL E. GAGNON, KARL F. KEIRSTEAD,[2] AND DONALD YAMASAKI[3]

ABSTRACT

Methods for determining sulphate acid ester in unstabilized cellulose nitrate have been studied. They were first verified by being applied to determine the sulphate acid ester in cellulose sulphate, cellulose acetate sulphate, and cellulose nitrate sulphate. Results showed that the sulphate ester in unstabilized cellulose nitrate can be determined satisfactorily by titration in water, or determination of calcium after ion exchange, or hydrolysis in acetone/water, or determination of sulphate after treatment with 50% alcohol.

INTRODUCTION

Various ion exchange methods for the estimation of sulphate acid ester in cellulose acetate sulphate were described in a previous paper (4). The acid ester RSO_4H was determined by titrating the acid released after ion exchange with calcium chloride solution or by determination of the exchanged calcium. The values for the sulphate ester by the hydrogen ion method were 3–40% below the gravimetric sulphate values. The low values were apparently due to adsorption of hydrogen ions on the sample because the determination of calcium and sulphate gave values that agreed within the limits of experimental error. In a recent publication (3), it was shown that the sulphate ester could be determined satisfactorily by titration in acetone/water solution before and after hydrolysis. The results indicated that the ester RSO_4H was titrated before hydrolysis and that sulphuric acid was titrated after hydrolysis. The sulphate content of crude but well-washed cellulose nitrate prepared from mixed acid varies from about 0.2 to 1.0% (expressed as H_2SO_4) according to the composition of the nitric–sulphuric acid. The form of this sulphate and the nature of the stabilization process have been somewhat obscure until quite recently. Two studies showing the presence of sulphate ester in unstabilized cellulose nitrate have led to a working hypothesis of the stabilization process. Kullgren (5) was the first apparently to produce

[1]*Manuscript received September 13, 1956.*

Contribution from the Department of Chemistry, Laval University, Quebec, Quebec, with financial assistance from the Defence Research Board of Canada.

[2]*Present address: Lignosol Chemicals Limited, Quebec, Quebec.*

[3]*Research assistant, Laval University. Present address: Canadian Industries Limited, McMasterville, Quebec.*

clear evidence for the presence of sulphate ester in unstabilized cellulose nitrate. Ion exchange studies showed that 12.57% *N* cellulose nitrate contained about three times as much sulphate acid ester as 13.05% *N* cellulose nitrate, although the total sulphate content was about the same in both types of cellulose nitrate. Without offering direct evidence Kullgren suggested that the excess of total sulphate over the sulphate ester value was due to the neutral ester R_2SO_4. Unpublished work done by Smith in the Nobel Laboratories of Imperial Chemical Industries Ltd. has been summarized recently by Miles (6). Studies were made on unstabilized cellulose nitrate in the complete range of nitrogen content. The total sulphate content of washed materials containing 9.5 to 13.5% nitrogen was estimated and the sulphate ester was determined by titration in acetone solution. The 13.4% *N* cellulose nitrate contained almost no acid ester whereas 10.7% *N* cellulose nitrate contained 0.52% sulphate ester (calculated as H_2SO_4). Contrary to Kullgren, it was thought that the sulphate not titrated in acetone was free H_2SO_4, imprisoned by physical means in areas of the cellulose structure inaccessible to water. The present paper describes methods that have been used to determine the sulphate ester content of a variety of cellulose nitrates. Where possible the sulphate ester has been estimated by two different methods. Attempts were made to assess the validity of the analytical methods by applying them to some analogues of unstabilized cellulose nitrate. Cellulose sulphate, cellulose acetate sulphate, and cellulose nitrate sulphate were used for this purpose.

EXPERIMENTAL

Cellulose Sulphate

Purified wood cellulose (3) (1 part) was treated with distilled water (15 parts) for 2 hours. After it had been centrifuged the cellulose was treated with glacial acetic acid (15 parts) for another 2 hours and again centrifuged. Each time the sample was centrifuged to about one and one-half times its original weight. The cellulose was then covered with a mixture (15 parts) of sulphuric acid (5%) in glacial acetic acid. After 2 hours the acid mixture was removed by suction and the residue was washed five times with water. The total sulphate present was determined as barium sulphate (4). The sulphate ester present was determined by ion exchange with calcium chloride, the calcium being estimated by titration with standard ethylenediaminetetraacetic acid (4). Total sulphate: 1.29% H_2SO_4. Sulphate ester: 1.34% H_2SO_4.

Cellulose Nitrate Sulphate

Cellulose sulphate as prepared above was converted to the salt form by several treatments with a dilute solution of sodium chloride. After being dried *in vacuo* for two days the cellulose sulphate was added to an acid mixture (50 parts) containing nitric acid (20.0%), sulphuric acid (63.0%), and water (17.0%). After 1 hour most of the acid was removed by suction and the crude fibrous product was added in portions with stirring to water. Found by nitrometer: N, 12.92%. Dry cotton linters nitrated with the same mixed

acid produced a cellulose nitrate containing 13.0% N. Total sulphate: 0.96% H_2SO_4. Sulphate ester: 0.62% H_2SO_4. Reference to Table II shows that both the total sulphate and the sulphate ester content are considerably higher than that normally found in cellulose nitrate containing 13.0% N.

Cellulose Nitrate

Cellulose (30 gm., 1 part) was dried for 1 hour at 105° C. and then placed in a desiccator until used. The dry cellulose was treated for 1 hour with a mixture (1500 gm., 50 parts) consisting of nitric acid (10.0%), sulphuric acid (70.0%), and water (20.0%). The mixed acid was analyzed by standard methods. The highest temperature reached during the nitration was 29° C. After most of the acid had been removed by decanting and by suction, the crude cellulose nitrate was added in portions to an excess of distilled water. The highest temperature reached during this addition was 39° C. Cellulose nitrate from cotton linters: N, 9.0%. Cellulose nitrate from wood cellulose: N, 8.5%; total sulphate, 1.62% as H_2SO_4; sulphate ester by hydrolysis method, 0.98% as H_2SO_4. Nitrogen was determined by the Devarda method.

Hydrolysis of Sulphate Ester Groups in Unstabilized Cellulose Nitrate

As previously described (4) all samples were washed continuously with distilled water that had been passed through an ion exchange column. The samples were used as soon as possible after being washed for 48 hours. A sample was removed from the washing apparatus and dried to about 50% water content by centrifuging. Portions were set aside for moisture, nitrogen, and sulphate determinations (3). Duplicate samples of moist cellulose nitrate (about 4 g. dry weight) were dissolved in acetone (700 ml.) and placed in a constant temperature bath at 25±0.1° C. The starting time was taken when half the solvent had been added. Aliquots were removed at intervals and the reaction stopped by dilution with an equal volume of water. The acidity was determined by titration with 0.01 *N* potassium hydroxide and was measured with a Macbeth pH meter. The end point determined from the plotted titration curve was usually at pH 6.5. The values for hydrolysis were the averages of determinations on duplicate samples.

RESULTS AND DISCUSSION

Reference has been made previously to the ion exchange method of determining the sulphate ester of cellulose acetate sulphate.

This method (4) involved the following steps: treating the sample with several portions of 0.02 *N* calcium chloride, washing it, and finally titrating the combined filtrates. In an attempt to improve the accuracy of the titration method, the sulphate ester was determined in the present work by direct titration of a well-stirred mixture of the sample in water with standard sodium hydroxide. As before (4), hydrolysis of the acetate or nitrate was minimized by completing the titration within 10–20 minutes. Results for the titration of cellulose sulphate, cellulose acetate sulphate, and cellulose nitrate sulphate are shown in Table I.

TABLE I

COMPARISON OF THE GRAVIMETRIC AND TITRIMETRIC METHODS OF DETERMINATION OF SULPHATE ESTER

Expt.	Sample	Sulphate ester, % H_2SO_4		Per cent difference
		Gravimetric	Titrimetric	
1	Cellulose sulphate	2.00	1.78	−11.0
2	Cellulose sulphate	1.40	1.52	+ 8.6
3	Cellulose sulphate	1.27	1.15	− 9.5
4	Cellulose sulphate	0.51	0.52	+ 2.0
5	Cellulose acetate sulphate	3.88	3.65	− 5.9
6	Cellulose acetate sulphate	3.15	3.52	+11.7
7	Cellulose acetate sulphate	2.23	2.29	+ 2.7
8	Cellulose acetate sulphate	2.20	2.50	+ 7.7
9	Cellulose acetate sulphate	2.15	2.29	+ 5.8
10	Cellulose nitrate sulphate	0.62*	0.555	−10.5
11	Cellulose nitrate sulphate	0.61*	0.61	0.0

*Calcium value.

All values for the sulphate ester by the previous procedure (4) were below the corresponding gravimetric values, the average percentage difference being 14. Examination of the data in Table I shows a high positive correlation (Rank-correlation coefficient = 0.985) (2) between the gravimetric and titration values. The cellulose nitrate sulphate contained some free sulphuric acid, which was evident from the excess of the gravimetric value over the calcium value for the sulphate ester. After a correction is made in the titration value for the free sulphuric acid, there is good agreement between the calcium value for the sulphate ester and the corrected titration value (Expt. 10 and 11, Table I).

When unstabilized cellulose nitrate samples were titrated in water under the same conditions with 0.01 *N* sodium hydroxide (Table II), it became

TABLE II

DETERMINATION OF SULPHATE ESTER IN UNSTABILIZED CELLULOSE NITRATE

Expt.	N, %	Gravimetric sulphate, % H_2SO_4	Titrimetric ester, % H_2SO_4	Sulphate ester, % of total sulphate
1	13.0	0.46	0.07	15.2
2	13.0	0.37	0.12	32.4
3	13.0	0.40	0.10	25.0
4	12.9	0.31	0.07	22.6
5	12.9	0.17	0.06	35.0
6	12.7	0.35	0.15	43.0
7	9.0	2.26	1.76	70.0
8	8.9	1.10	0.93	84.5
9	8.4	2.82	2.05	72.8

clear that contrary to the behavior of the cellulose nitrate sulphate in Expt. 10 and 11, Table I, little or no free sulphuric was being titrated. This was evident because the titration values were lower, not higher, than the corresponding gravimetric values. Since we use 98 for the equivalent weight of RSO_4H

expressed as H_2SO_4, the ester plus one half of the free acid gives a value equal to the gravimetric sulphate value.

Referring to Expt. 2, Table II, the titration value for the sulphate ester was 0.12%. In the same experiment the calcium value for the sulphate ester, not shown in the table, was found to be 0.10%. The agreement between these two values is a good indication that the titration value is a satisfactory estimate of the sulphate ester but there may be a constant error of +10 to +20%.

From later experiments it is estimated that about one half the free acid can be titrated when the titration is done very slowly. The sample in Expt. 5 was a duplicate of the sample used in Expt. 4 and was boiled in water for ½ hour and then washed. The loss in sulphate seems to be mainly free acid. In agreement with the work reported by Miles (6) the total sulphate and the proportion of sulphate ester tend to increase with decreasing nitrogen content.

Some typical values for the sulphate ester by the calcium method are shown in Table III where the cellulose nitrate samples have a nitrogen con-

TABLE III

DETERMINATION OF SULPHATE ESTER IN UNSTABILIZED CELLULOSE NITRATE

Expt.	N, %	Sulphate, % H_2SO_4		Sulphate ester, % of total sulphate
		Gravimetric	Calcium	
1	13.1	0.60	0.024	4.0
2	13.0	0.50	0.012	2.5
3	12.9	1.00	0.14	14.0

tent ranging from 12.9 to 13.0%. The sulphate ester values are somewhat lower than those for similar samples shown in Table II.

One step in the commercial stabilization of cellulose nitrate is milling, also termed pulping or beating. According to Davis (1), the milling treatment washes out residual acid from the fibers. According to this explanation, the proportion of sulphate ester would increase during the milling treatment and the final sulphate value might be a measure of the sulphate ester content. There is no reason to think that the sulphate ester would be affected by a mechanical treatment. The results obtained from the milling of unstabilized cellulose nitrate and analogous compounds are shown in Table IV. No loss in sulphate occurred in cellulose acetate sulphate and cellulose nitrate sulphate where the sulphate was entirely in the ester form. A considerable loss in sulphate occurred in the cellulose nitrate but the sulphate ester content as determined by the calcium method remained constant.

In each experiment the discrepancy between the final gravimetric sulphate and the sulphate ester seems to be greater than the probable experimental error. Hence it does not appear likely that all unbound sulphate can be removed by this treatment.

The kinetics of the hydrolysis of the sulphate ester of cellulose acetate

TABLE IV

THE EFFECT OF MILLING ON THE SULPHATE ESTER CONTENT

Expt.	Sample	N, %	Milling time, min.	Sulphate, % H_2SO_4		Sulphate ester, % of the total sulphate
				Total gravimetric	Ester calcium	
1	Cellulose acetate sulphate	—	Nil	1.58	1.58	100
			5	1.56	—	—
2	Cellulose nitrate sulphate	12.9	Nil	1.14	1.14	100
			120	1.16	—	—
3	Cellulose nitrate	13.0	Nil	0.50	0.14	28.0
			5	0.13	0.10	77.0
4	Cellulose nitrate	12.6	Nil	1.16	0.48	41.4
			5	0.66	0.48	72.8
5	Cellulose nitrate	13.0	Nil	0.88	0.24	27.3
			300	0.50	0.24	48.0

sulphate in acetone/water was studied recently by Gagnon *et al.* (3). A similar hydrolysis was found for cellulose nitrate sulphate and some samples of unstabilized cellulose nitrate.

A brief consideration shows that a number of interesting possibilities regarding the sulphate content can be studied by this method. If the sulphate content is entirely the acid ester, as in cellulose acetate sulphate, the initial titration value will be one half the final titration value obtained from complete hydrolysis of RSO_4H to H_2SO_4. A mixture of free H_2SO_4 and RSO_4H will give an initial titration greater than one half the final titration value, the difference of the two values being a measure of the sulphate ester. If the neutral ester suggested by Kullgren is present, the initial value will be less than one half the value calculated from the sulphate content. With hydrolysis of the neutral ester, the final titration value will again correspond to the total gravimetric value. Without hydrolysis of the neutral ester, the final titration value will be less than the value expected from the total gravimetric value.

The acetone/water hydrolysis method was applied in the present work to the cellulose nitrate sulphate samples.

As before (3), moist duplicate samples were dissolved in acetone and aliquots were titrated in acetone/water at suitable intervals. A considerable increase in acidity occurred with an increase in the time of hydrolysis.

The initial titration value was greater than one half the final titration value thus showing the presence of a mixture of free H_2SO_4 and ester RSO_4H in the original sample. As shown in Table V there is good agreement between

TABLE V

HYDROLYSIS OF SULPHATE ESTER GROUPS IN UNSTABILIZED CELLULOSE NITRATE SULPHATE IN ACETONE/WATER

Expt.	Sulphate, % H_2SO_4		Ester, % H_2SO_4	
	Gravimetric	Final titrimetric	Calcium	Hydrolysis
1	0.667	0.672	0.480	0.480
2	0.525	0.495	0.302	0.314
3	0.480	0.460	0.308	0.350

the gravimetric sulphate and the sulphate determined from the final titration value. A similar agreement is found between the sulphate ester content determined by the calcium method and by the increase in acidity.

Some preliminary results for the hydrolysis of unstabilized cellulose nitrate are shown in Table VI. Again there is fairly good agreement between the

TABLE VI

HYDROLYSIS OF SULPHATE ESTER GROUPS IN UNSTABILIZED CELLULOSE NITRATE IN ACETONE/WATER

Expt.	Hydrolysis, hr.	N, %	Sulphate, % H_2SO_4		Ester, % H_2SO_4
			Grav.	Final hydrolysis	
1	24	10.8	1.90	1.80	0.81
2	24	10.5	0.50	0.45	—
3	22	9.0	—	2.26	1.98
4	20	8.5	1.62	1.30	0.98

gravimetric values and the titration value at the end of the hydrolysis. No hydrolysis was detected in some cellulose nitrate samples in the range 13.0–13.5% N. The low sulphate ester content of these samples (Table II) makes it most unlikely that convincing evidence for hydrolysis could be obtained by this method.

A 50% solution of ethanol is often used in the laboratory to stabilize a sample of crude cellulose nitrate by removing most of the sulphate present. It was of interest to investigate the possibility that the alcohol may release free acid by swelling the fibers without affecting the acid.

The data in Table VII show that the final sulphate content after treatment with 50% alcohol corresponds to the ester content. The ester determination was done on a similar but untreated sample because it was found that con-

TABLE VII

EFFECT OF 50% ALCHOL ON SULPHATE ESTER GROUPS IN CELLULOSE DERIVATIONS AT 34° C.

Expt.	Sample	Time, hr.	Sulphate, % H_2SO_4		
			Initial gravimetric	Final gravimetric	Calcium ester
1	Cellulose sulphate	22	1.27	1.26	1.27
2	Cellulose nitrate sulphate	20	1.07	0.73	0.61
3	Cellulose nitrate (13.2 % N)	20	0.14	0.06	0.06
4	Cellulose nitrate (12.9 % N)	48	0.90	0.16	0.15

siderable absorption of calcium occurred after treatment with alcohol. The effect of absolute alcohol was more drastic. When cellulose sulphate was treated with absolute alcohol for 22 hours at 34° C., 66% of the sulphate was removed. It was observed previously (3) that the rate of hydrolysis of the

sulphate ester of cellulose acetate sulphate increased markedly with a decrease in the water concentration of the acetone/water.

The stability of the sulphate ester during the drying process is shown in Table VIII. The sulphate ester was split off when cellulose sulphate, cellulose

TABLE VIII

STABILITY OF THE SULPHATE ESTER DURING THE DRYING PROCESS

Expt.	Sample	Sulphate, meq./100 g.		Decomposition, %
		Initial titration	Final titration	
1	Cellulose sulphate	16.4	35.2	100
2	Cellulose acetate sulphate	31.5	65.1	100
3	Cellulose nitrate sulphate	8.5	16.6	98

acetate sulphate, and unstabilized cellulose nitrate were dried in a vacuum (4). The initial titration value was calculated from the gravimetric sulphate value and the final titration value was obtained when the sample, after it had been dried, was titrated in water. This method could not be used to determine the stability of the sulphate ester in unstabilized cellulose nitrate because extensive decomposition of the nitrate ester took place.

However, the data of Table VIII suggest that the sulphate ester in unstabilized cellulose nitrate would also split off when the material is dried.

REFERENCES

1. DAVIS, T. Chemistry of powder and explosives. John Wiley & Sons, Inc., New York. 1943.
2. DIXON, W. J. and MASSEY, F. J. Introduction to statistical analysis. McGraw-Hill Book Co., Inc., New York. 1951.
3. GAGNON, P. E., KEIRSTEAD, K. F., WALKER, J., and KAVANAUGH, K. Can. J. Technol. 34: 71. 1956.
4. KEIRSTEAD, K. and MYERS, J. Can. J. Chem. 32: 566. 1954.
5. KULLGREN, C. Ing. Vetenskaps Akad. Handl. No. 165. 1942.
6. MILES, F. D. Cellulose nitrate. Clarke, Irwin & Co. Ltd., Toronto. 1955.

THE DESIGN AND OPERATION OF A CLOUD CHAMBER[1]

By Louis A. Madonna

ABSTRACT

The design and operation of an expansion type cloud chamber is discussed. The difficulty in most cloud chambers is that the carrier gas is impure and therefore the condensation achieved is heterogeneous. The entire design and operational objective of this chamber was to obtain homogeneous nucleation and growth of water droplets. An equation is also given relating the initial temperature of the saturated pure nitrogen gas to the temperature at which water vapor is condensed homogeneously.

I. PURPOSE OF PAPER

The purpose of building the cloud chamber was to study the critical supersaturations of water vapor at various low temperatures. This paper has been written to show the difficulties arising in cloud chamber design and construction. An equation is also developed relating the original temperature of vapor and the temperature at which droplets first form on supercooling that vapor.

II. THE DESIGN OF THE APPARATUS

The design of a cloud chamber is governed by the concentration of second phase impurities tolerated. In our apparatus we desired to have the concentration of these impurities at a minimum.

A flow sheet of the apparatus is shown in Fig. 1 and a photograph on Fig. 2. The gas or "carrier gas" used was prepurified nitrogen supplied by the

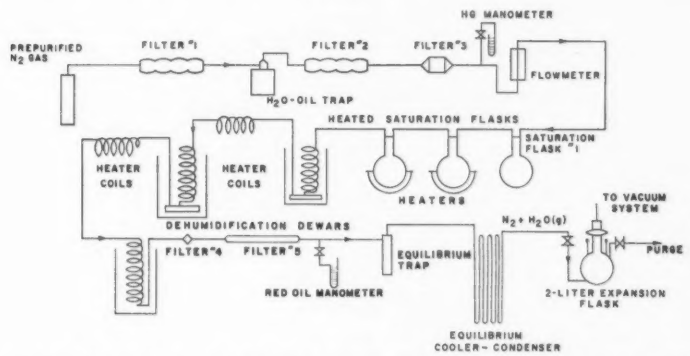

Fig. 1. Gas flow system. All tubing is 7 mm. pyrex that has been fused together. No rubber connections have been used.

[1]*Manuscript received October 22, 1956.*

Contribution from the Department of Chemical Engineering, University of Ottawa, Ottawa, Canada. The research described in this paper was sponsored by the Geophysics Research Division, Air Force Cambridge Research Center, Cambridge, Mass., under contract No. A.F. 19(122)-185.

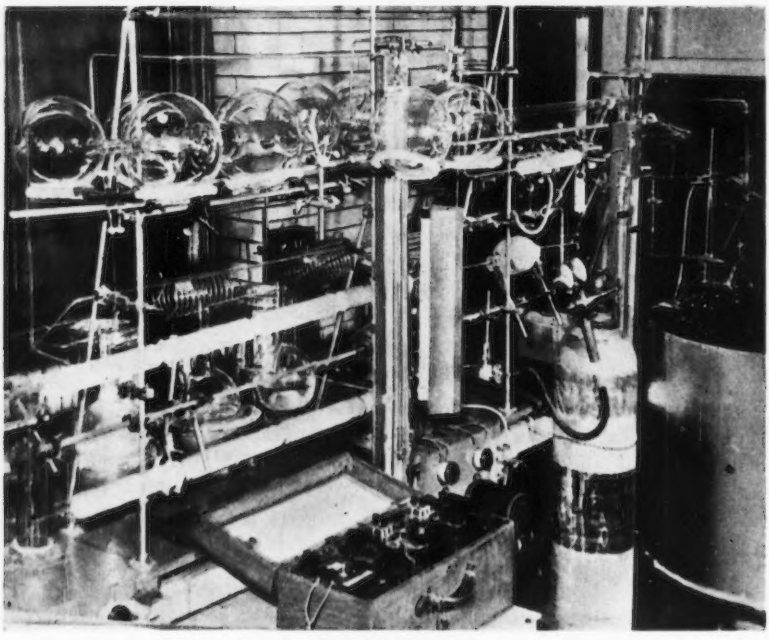

FIG. 2. Photograph of apparatus.

Air Reduction Company. The gas was fed into a 4ft. long, glass wool packed filter (Filter No. 1) which removes coarse dirt particles from the gas. The gas then entered the water-oil trap, which consisted of a regular re-entrant tube vapor trap submerged in an acetone – dry ice mixture. The next unit was a tight-packed glass wool filter (Filter No. 2) in which the gas was further purified. The gas then passed through a bacteriological filter and then to a flowmeter. The flowmeter was calibrated to give readings in liters per minute of gas flowing.

In order to obtain pure water vapor three saturation flasks half filled with water were inserted in the system. The last two flasks were heated to ensure sufficient water vapor removal by the carrier gas. The gas plus water vapor was sent through a "condensation train" which was arranged in a manner to cause a condensation of all water vapor not in equilibrium with water (or ice) at 0° C. The deposition of water vapor into the liquid state was caused by surface protuberances and tube bends. The coils between the Dewars were used to evaporate small droplets and also to catch any large drops that were formed in the condensation process. As an added precaution Filters No. 4 and No. 5 were put into the system.

An equilibrium trap in our refrigerated bath adjusted the partial pressure of the water vapor so that it was approximately equal to the vapor pressure of water at the bath temperature. The equilibrium condenser cooled the gas further owing to its large heat transfer surface and therefore the partial

pressure of the water vapor was made equal to the vapor pressure of the water at the bath temperature. The line between the condenser and the expansion flask was made as short as possible and also it was heavily insulated. As an added precaution the sample of gas and water vapor was allowed to remain in the expansion flask for 15 minutes before an expansion was attempted.

The expansion flask itself is shown in Fig. 3. It was made so that the viewing

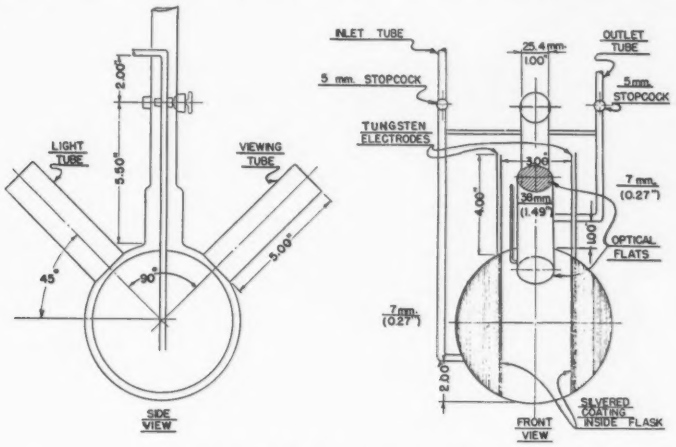

FIG. 3. Two-liter expansion flask.

of the flask interior and the lighting of the interior could be done well above the surface of the heat transfer liquid. Optical flats were used in the viewing and lighting tubes. To remove ions in the gas sample two opposite non-contacting areas in the inside of the flask were coated with silver. Tungsten electrodes extended into the expansion flask and were connected through a Wood's metal seal to the silvered areas.

The expansion flask was connected to a two-stage vacuum system. The system is shown in Fig. 4.

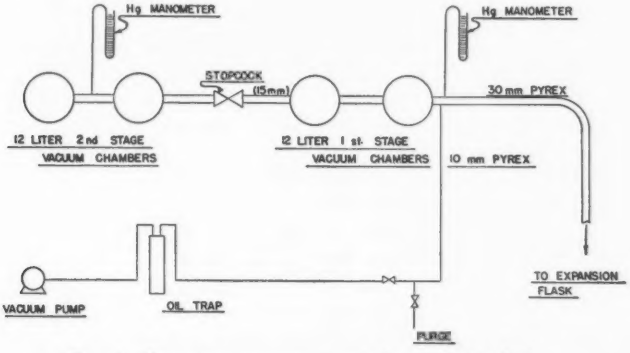

FIG. 4. Two-stage vacuum system for expansion flask.

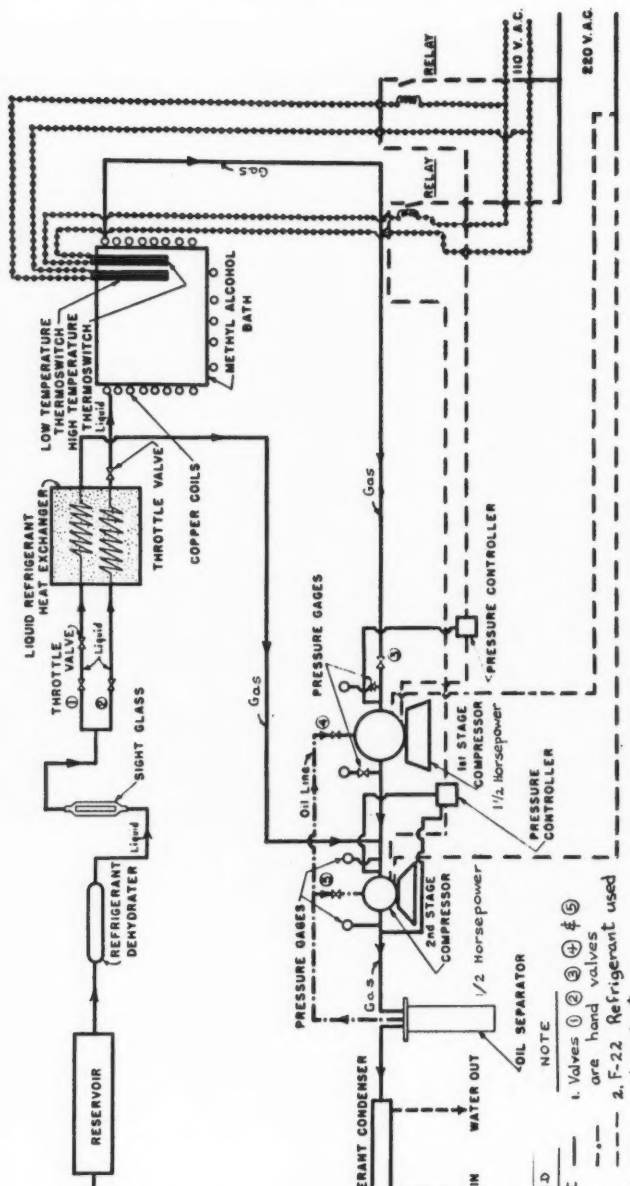

FIG. 5. F-22 refrigeration system.

III. THE REFRIGERATION SYSTEM

The equilibrium trap, equilibrium coils, and the expansion flask were all kept at a constant ($\pm 0.02°$ C.) low temperature ($+10$ to $-80°$ C.) by immersion in a refrigerated methanol bath. The 30-gallon bath was heavily insulated and well agitated to ensure temperature uniformity throughout the volume. A diagram of the Freon-22 refrigeration system and the low temperature thermostat bath is given in Fig. 5. Fig. 6 is a photograph of this apparatus.

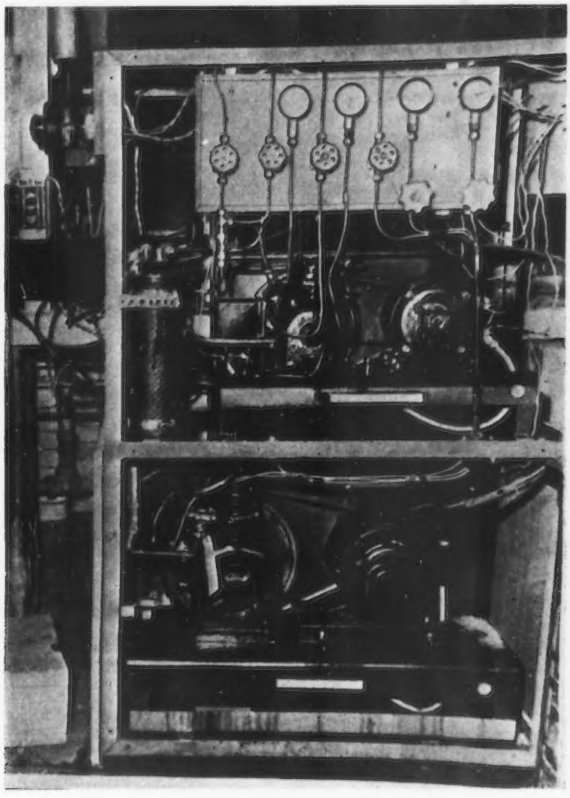

FIG. 6. Photograph of refrigeration system.

Operation of the refrigeration system is as follows: F-22 refrigerant gas from the cooling coils which are imbedded in the walls of the thermostat bath is compressed in two stages. The compressed gas is passed through an oil separator to a water-cooled condenser where it is condensed to a liquid. This liquid flows to a reservoir and from there flows through a dehydrator and a sight glass to the liquid refrigerant heat exchanger. Before entering this exchanger, the liquid is separated into two streams by means of valves

1 and 2. The first stream is throttled to a low temperature and serves to cool the second stream (unthrottled liquid) as they pass through the exchanger concurrently. The throttled stream is warmed in the exchanger and emerges as a gas which is passed to the intake of the second stage compressor. The cooled liquid stream emerging from the exchanger is throttled to a low temperature and is passed to the coils of the thermostat bath where it evaporates, providing refrigeration.*

Temperature control is obtained with Fenwal inverse thermoswitches that activate relays which start and stop the compressors. For bath temperatures down to −50° C., the first stage compressor is put on control. For bath temperatures between −50° C. and −80° C., the second stage compressor runs continuously and the first stage compressor is on control. Each compressor is equipped with a pressure controller as a safety device that will shut off the motor if the pressure should become excessive.

Using this above procedure the bath temperature was controlled to ±0.1° C. A later refinement was to insert immersion heaters in the bath and keep the refrigeration system running continuously. The heat input was adjusted with Variacs and the control was to ±0.02° C. Absolute temperatures in the bath were measured to ±0.02° C. by means of a carefully calibrated, 5-strand copper–constantan thermocouple and a Leeds and Northrup K-2 potentiometer.

IV. OPERATION

A. Set-up and Purging Procedures

The refrigerated bath was set to control at some desired temperature. The electric heaters under the saturation flasks were set so that the water in the flask came to a temperature of about 70–80° C. If the bath was to be operated below 0° C., ice was put in the three condensation Dewars. Dry ice was placed in the water–oil trap. The nitrogen (or other carrier gas) gas was then admitted into the system until the pressure on the mercury manometer was positive by 20–30 mm. of mercury. When this value had been reached, it was safe to first open the entrance stopcock to the expansion flask. The exit stopcock could then be opened providing that the flask and the system were at a positive pressure of 20–30 mm. of mercury. This above procedure eliminated any danger of the flask drawing in dirty air owing either to a possible temperature decrease since the last operation or a slight vacuum left from a previous expansion of the gas into the vacuum system. The flow of the gas through the system or "purge" was continued for about 10 minutes. After this length of time the flask had a fresh sample of gas plus water vapor without any suspended droplets from a previous expansion.

Calculation of the Necessary Purge Time

The time of purge was determined in the following manner. Prepurified nitrogen gas flowed into the expansion flask at a rate of 1 liter per minute

**The refrigeration unit was designed and constructed by Refrigeration Services Incorporated of Pittsburgh, Pennsylvania.*

(1000 cu. cm. per min.). In the 2-liter flask the impurity (droplets) was present at a certain weight. Let x = weight of impurity in the flask at the end of "t" minutes. The concentration of impurity or possible active centers per cubic centimeter is then

[1] $$c = x/2000.$$

In the time dt, 1000 dt cu. cm. of moist nitrogen came in and 1000 $c\,dt$ grams of impurity went out. The change of active centers is expressed by

[2] $$dx = -1000\,c\,dt$$

or putting equation [1] into [2]

$$dx = -1000/2000\,x\,dt$$

[3] $$dx/x = -\tfrac{1}{2}\,dt \quad .$$

Equation [3] is the differential equation relating the decrease of impurity in the flask with the increase of time. Integrating [3]:

$$\int_{x=x_1}^{x=x_2} dx/x = -\tfrac{1}{2} \int_{t=0}^{t=t} dt$$

Now by letting:

[4] $$\ln(x_2/x_1) = -\tfrac{1}{2}\,t,$$

d = density of active centers,

v = volume of each active center,

also let $$n = \frac{\text{total weight of centers in the flask}}{\text{weight of one active center}},$$

then n = number of centers in flask.

For initial and final conditions, 1 and 2 respectively:

$$x_1 = n_1 v_1 d_1,$$
$$x_2 = n_2 v_2 d_2.$$

Since most of the centers are of the same density and are all of approximately the same volume:

$$v_1 = v_2$$
$$d_1 = d_2$$
$$\therefore\ x_2/x_1 = n_2/n_1.$$

Substitution of the number ratio for the weight ratio in [4] gives

$$\ln(n_2/n_1) = -\tfrac{1}{2}\,t$$

[5] $$\text{or } t = 4.6 \log_{10} (n_1/n_2)\ .$$

Assuming that the residual concentration of droplets after expansion is about 1000 droplets/flask and the desired lower limit is a maximum of 10 droplets/flask, then equation [5] gives:

$$t = 4.6 \log_{10} (1000/10)$$
$$t = 9.2 \text{ minutes.}$$

The value of 1000 is very high, for experiments usually left about 100 droplets as a maximum value. A purge time of 10 minutes was used.

B. Equilibrium Time

After the gas had purged out the flask for 10 minutes the stopcock in the entrance line was closed while the exit line stopcock was left open for about 10–15 seconds. The exit stopcock was then closed. This procedure was followed in order that the gas sample trapped in the flask would be at atmospheric pressure. The gas plus water vapor was then allowed to remain in the flask for 15 minutes prior to the expansion.

C. Temperature Decrease in Flask Due to Expansion of Gas

In order to cause a temperature decrease and therefore condensation in the expansion flask, the vacuum system was set to some pressure lower than atmospheric pressure. When the stopcock separating the expansion flask and the vacuum system was opened there was a temperature decrease in the flask caused by some of the gas rushing out of the flask into the vacuum system. If we can assume that the expansion is reversible and adiabatic then we can calculate the final temperature after expansion. This assumption is valid, for with apparatus very similar to the one presented in this paper Makower (1) calculated the specific heat ratios, C_p/C_v, for several gases. These check fairly well with calorimetric work done by Scheel and Heuse (3, 4, 5).

Gas	W. Makower (about 18° C.)	Scheel and Heuse
Air	1.4025	1.401 (20° C.)
Oxygen	1.3977	1.399 (20° C.)
Carbon dioxide	1.2995	1.30 (20° C.)
Hydrogen	1.4084	1.407 (16° C.)

The method of calculation of our final temperature is identical with that of Makower.

Equation Relating Temperatures and Pressures in the System

The gas in the flask can be assumed to be ideal since it is at atmospheric pressure. Therefore the reversible adiabatic formula can be used in order to obtain the temperature after expansion of the gas:

$$[6] \qquad T_2/T_1 = (P_2/P_1)^{(k-1)/k};$$

T_1 = temperature of gas before expansion (or of bath),
T_2 = temperature of gas immediately after expansion,
P_1 = pressure in flask before expansion (atm. pressure),
P_2 = pressure in flask after expansion,
C_p = specific heat at constant pressure of nitrogen,
C_v = specific heat at constant volume of nitrogen,
$k = C_p/C_v$.

The partial pressure of the water vapor exerts a negligible effect on k. This can be shown by using the following equation proposed by Richarz (2):

[7] $$1/k-1 = \frac{P_{N_2}}{P(k_{N_2}-1)}+\frac{P_{H_2O}}{P(k_{H_2O}-1)};$$

P = atmospheric pressure,
P_{H_2O} = partial pressure of water vapor,
P_{N_2} = partial pressure of nitrogen,
k, k_{N_2}, k_{H_2O} = specific heat ratios for gas mixture, nitrogen, and water respectively.

If the maximum temperature of operation of our chamber is taken as a basis then a calculation can be made showing the magnitudes involved.

At 20° C. the vapor pressure of water = 17.53 mm. Hg. Average barometric pressure = 760 mm. Hg,

$$\frac{1}{k-1} = \frac{760-17.53}{760(k_{N_2}-1)}+\frac{17.53}{760(k_{H_2O}-1)}.$$

The water vapor term can be neglected as the value is negligible. It can be seen in Fig. 7 that k_{N_2} does not change greatly with temperature. An

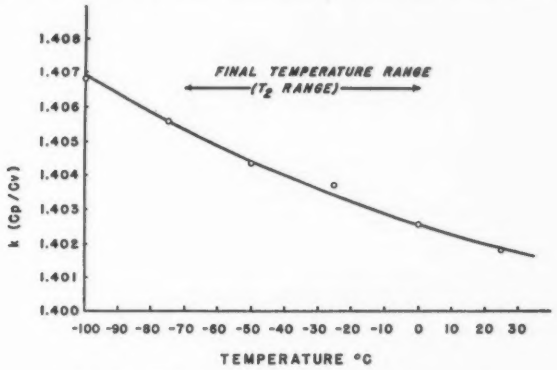

FIG. 7. Plot of k versus temperature (nitrogen).

average value of 1.403 was assumed appropriate for the experimental range covered.

D. Criterion on the Type of Condensation Produced in the Cloud Chamber

A sample of nitrogen gas and water vapor when chilled can result in either homogeneous or heterogeneous condensation. Homogeneous condensation occurs when no foreign particles are present upon which the water vapor can deposit. Heterogeneous condensation occurs when:

1. Small particles are present in the gas sample.
2. Aggregates of the condensing substance remain from a previous condensation.

Ions also affect the temperature of condensation; this effect will be discussed in a later publication.

It is easily proved which type of condensation exists in a cloud chamber.

A very slight chilling (two to three degree centigrade temperature drop) in a heterogeneous system will cause profuse condensation; homogeneous condensation only occurs if the temperature decrease is 15° C. or more.

E. Relationship between Original Temperature of Water-saturated Pure Nitrogen Gas and Temperature of Incipient Condensation of Water Droplets

Water vapor and pure nitrogen gas samples were set at various initial temperatures and their condensation temperatures calculated when the first evidence of deposition was revealed in the expansion flask. When T_1 versus T_2 was plotted for points of incipient condensation of water droplets, the resulting curve was a straight line. This is shown in Fig. 8. The equation

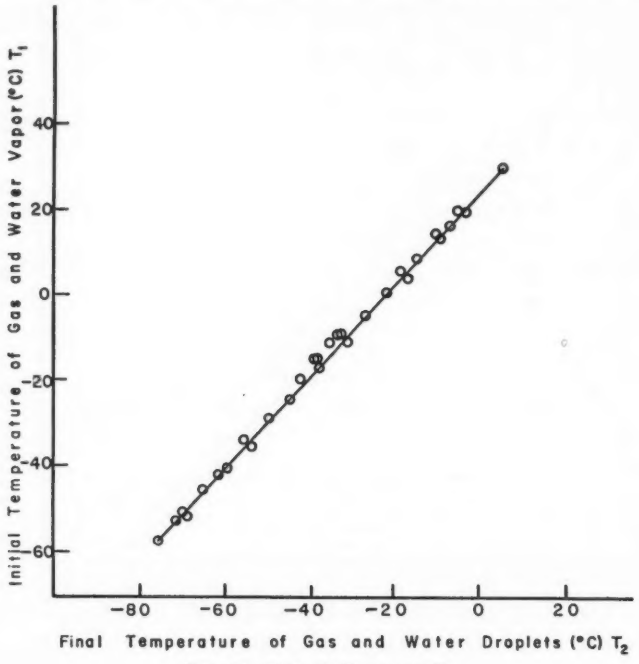

FIG. 8. Plot of T_1 versus T_2.

for the straight line is

$$T_2 = 0.933T_1 - 23.34. \quad [8]$$

Equation [8] relates the final lower temperature (T_2) necessary to condense water vapor into droplets from a nuclei-free saturated sample at a given initial temperature, T_1.

REFERENCES

1. MAKOWER, W. Phil. Mag. 5: 226. 1903.
2. RICHARZ, F. Ann. Physik, 19: 457. 1908.
3. SCHEEL, K. and HEUSE, W. Ann. Physik, 37: 79. 1912.
4. SCHEEL, K. and HEUSE, W. Ann. Physik, 40: 473. 1913.
5. SCHEEL, K. and HEUSE, W. Ann. Physik, 59: 86. 1919.

NICKEL–CADMIUM BATTERIES

II. IMPREGNATION OF POSITIVE PLATES BY THERMAL DECOMPOSITION OF AQUEOUS NICKEL NITRATE[1]

By P. L. Bourgault, Phyllis E. Lake, E. J. Casey, and A. R. Dubois

ABSTRACT

A method is described for placing electrochemically-active material in the pores of sintered nickel plaques. The plaque is first immersed in aqueous nickel nitrate; then the nickel nitrate in the pores is decomposed at high temperatures to an intermediate which converts rapidly to nickel hydroxide in caustic solutions. The effects of temperature and time of immersion and of thermal decomposition, and of the surrounding atmosphere, have been studied. Results on electrical behavior of the plates are presented, and a preliminary discussion of the mechanism of the impregnation process is offered.

INTRODUCTION

The commercial method for producing plates for nickel–cadmium batteries from sintered plaques (2, 4) is long and complex. The method here described for positive plates reduces the number of steps and replaces the objectionable polarization step by a thermal decomposition and chemical conversion. Conditions have been found by which the new method in five steps can produce positive sintered plates containing the same amount of active material as those formed by the commercial method in 16 steps. No attempt at cost analysis for either equipment or processing has been made.

EXPERIMENTAL MATERIALS AND METHODS

All chemicals were reagent grade and new solutions were used for each experiment. Carbonyl nickel plaques obtained from Clevite Corp. (0.025 in. thick) and Amplex Division, Chrysler Corp. (0.080 in. and 0.025 in. thick) were used.

The thermal impregnation process consists of five essential steps. These and the range of experimental conditions studied are contained in Table I. Within the ranges indicated some two hundred plates were made and tested in the survey.

Thermal decompositions were done in one of three ovens: Cenco, type 95050, range 25°–250° C.; Blue M Electric Co., type No. CW38, 35°–288° C.; Volta Mfg. Co., Muffle furnace, type BC44, 100°–2000° F.

For reduced pressure experiments the Cenco oven was fitted with a glass vacuum desiccator. The high pressure steam experiments were conducted within a steel bomb (equipped with the necessary thermocouples and pressure gauge) which was heated in a Westinghouse Industrial RF Generator, 5 kw., type CF813B.

[1]*Manuscript received November 6, 1956.*
Contribution from the Defence Research Chemical Laboratories, Ottawa, Canada. Issued as D.R.C.L. Report No. 209.

TABLE I

Step	Solution	Temperature range (°C.)	Time range (min.)	Remarks
1. Immersion	$Ni(NO_3)_2.6H_2O$ dissolved in water of hydration	(*a*) 85–115	120	Atmospheric pressure
		(*b*) 85–125	10	4 min. under reduced pressure, 6 min. atmospheric pressure (referred to as 10 min. vacuum)
2. Decomposition	—	100–500	10–1080	In air, N_2, steam at 1 atm., high pressure steam and vacuum
3. Conversion	1.3 sp. gr. KOH	75–85	60–960	16 hr. conversion time was used for convenience (overnight)
4. Washing	Distilled H_2O	25	~120	Until pH of drip ~7
5. Drying	—	75–85	~120	To constant weight

Plates were placed in test cells as in previous work (1). They were given three forming cycles after the manner suggested by Fleischer (2), an additional low rate discharge, and then a limited test program of discharges ranging between 0.0003 and 0.12 amp. cm.$^{-2}$

RESULTS AND DISCUSSION

Parameters of the Impregnation Process

Temperature and Time

In Fig. 1 is shown a typical set of theoretical capacities (based on weight gain during processing) plotted against decomposition temperature. Curves are given for 10 minutes, 1 hour, and 18 hours of decomposition. For each time investigated, there is an optimum temperature at which plates of highest theoretical capacity are produced.

Kano and Wakayama (3) have found that, on being heated at temperatures between 200° and 1100° C., $Ni(NO_3)_2.6H_2O$ decomposes to NiO. This breakdown might be written:

$$Ni(NO_3)_2.6H_2O \xrightarrow{\Delta} NiO+6H_2O+2NO_2+\tfrac{1}{2}O_2 \qquad [1]$$

although the stoichiometry has not been established. It was found in the present work that the NiO so formed in the sintered plaque is electrically inactive. However, it was found that if the nitrate is heated for moderate lengths of time at controlled temperatures (about 180–250° C. depending on the duration of the heating) the rate of decomposition falls essentially to zero as the material goes through an intermediate stage. The $Ni(NO_3)_2.6H_2O$ decomposes toward a solid whose weight is consistent with the formula $Ni(OH)NO_3$, and whose X-ray diffraction pattern is as yet unidentified but

which resembles the pattern ascribed to basic copper nitrate. This reaction might be written:

$$2\ Ni(NO_3)_2.6H_2O \xrightarrow{\Delta} 2Ni(OH)NO_3 + 2NO_2 + 5H_2O + \tfrac{1}{2}O_2 \quad [2]$$

The stoichiometry again is unknown. The intermediate, if immersed in hot aqueous KOH, was found to convert rapidly to electrically-active hydroxide, presumably $Ni(OH)_2$.

At temperatures well below the optimum, considerable amounts of the liquid $Ni(NO_3)_2.6H_2O$ are lost from the plaque during thermal decomposition because the outer layer is not decomposed quickly enough to seal the remainder in the plaque. Nitrate which has not been converted to intermediate during decomposition may be leached out or forced out physically during the conversion step. It was observed that the lower the decomposition temperature the greater the amount of material lost during decomposition and also the greater the amount of material lost during conversion.

At temperatures above the optimum (Fig. 1), a fraction of the material may

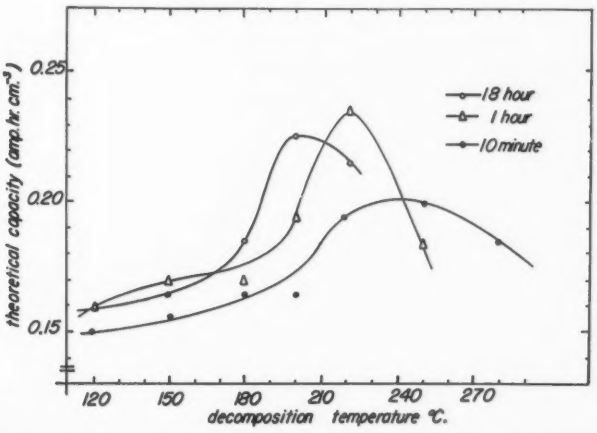

FIG. 1. Theoretical capacity of experimental plates as a function of decomposition temperature. Immersed at 90° C. for 2 hours at 1 atm. pressure.

be completely decomposed to the electrically-inactive NiO. It has been established that the optimum oven temperature for the decomposition within the sintered plate is lower than would have been predicted from decomposition curves taken on pulverized and spread nickel nitrate. Presumably the exothermic corrosion reaction of the nickel sinter raises the temperature of the plate, at least in spots, and thus forces the decomposition past the $Ni(OH)NO_3$ stage to NiO.

Amount of Nickel Impregnated into the Plaque during Immersion

The density of the "molten" nickel nitrate [$Ni(NO_3)_2.6H_2O$] was measured at 95° C. and found to be 1.77 g.cm.$^{-3}$ The plaques used were about 80%

porous, i.e. 80% free volume. Assuming that the electrochemical reaction within the positive plate is $Ni^{+2} \rightleftharpoons Ni^{+3} + e^-$, that the pores are completely filled during immersion, that no side reactions occur, and that no nickel is lost during subsequent processing, the maximum theoretical capacity of a plate can be calculated:

$$\frac{0.8 \times 1.8 \text{ g.cm.}^{-3} \times 96{,}500 \text{ amp. sec. equiv.}^{-1}}{290.8 \text{ g. equiv.}^{-1} \text{ Ni}(NO_3)_2 . 6H_2O \times 3600 \text{ sec. hr.}^{-1}} = 0.13 \text{ amp. hours cm.}^{-3}$$

Plaques which were given a 10-minute vacuum immersion at 100° and decomposed under reduced pressure so that the gaseous decomposition products were quickly removed had capacities very close to 0.13 AH cm.$^{-3}$ The results show that additional active material is introduced if the sinter is allowed to remain in contact with the oxidizing media of immersion and/or thermal decomposition for any appreciable time. Thus plaques immersed for 2 hours at 100° C., and decomposed under reduced pressure, had capacities of the order of 0.175 AH cm.$^{-3}$; and plaques given either the 2 hour – 100° immersion or the 10 minute – 115° vacuum immersion, and decomposed under atmospheric pressure such that the oxidizing agents, the nitrogen oxides, were slow to escape gave capacities of the order of 0.22 AH cm.$^{-3}$ These effects of time and temperature of immersion are shown by typical results listed in the following tables.

TABLE II

EFFECT OF IMMERSION TEMPERATURE ON CAPACITY OF PLATES (10 MIN. VAC.)

Immersion temp. (°C.)	Theor. cap. (AH cm.$^{-3}$)
64	0.16
95	0.19
115	0.22
120	0.22

TABLE III

EFFECT OF IMMERSION TIME AT 115° ON CAPACITY OF PLATES

Immersion time (min.)	Theor. cap. (AH cm.$^{-3}$)
2.25	0.195
10	0.22
40	0.247
110	0.273

It is very probable that the extra capacity placed in the plates by the longer immersion times and/or higher temperatures is directly or indirectly a result of oxidation of the nickel metal sinter by nitrate. However, if all the "excess" capacity were due to oxidation of the sinter alone, as high as 25% of the sinter would be oxidized. The physical appearance of the plate and the absence

of crumbling under electrical testing indicate that this is unlikely, and hence a second reaction which serves to concentrate the active material must exist. It is suggested that during the immersion step oxidation raises the pH within the pores and precipitates hydroxide or basic nickel salt within the pores. The results listed in the above tables indicate that both the oxidation and precipitation reactions slow down as the reaction products accumulate on the pore wall.

An important variable not studied in this work is the impurity content of the sintered nickel plaque; the oxidation rate would be expected to increase with increasing impurity content, thus increasing both the theoretical and the real capacity.

After concentrated immersion no active material is shed from the plaque during thermal conversion; during electrolytic conversion, material is shed. Thus the thermal method makes the concentrated immersion feasible.

Change of Atmosphere during Thermal Decomposition

Reduced pressure during thermal decomposition increases the rates of both reactions [1] and [2] by removal of the gaseous products, thus reducing the oxidation of the sinter and the consequent increase in capacity.

Attempts to produce electrically-active, nitrate-free product directly by decomposing the nitrate at high temperatures (300–600°) in a stream of dry steam, both at atmospheric and high pressures, were unsuccessful. Carrying out the decomposition in a nitrogen atmosphere had no effect on plate capacity. Apparently the gaseous decomposition products, NO_2 and water vapor, determine the atmosphere deep within the pores so that external changes of atmosphere have little effect.

Physical Properties of the Plaques

Since commercial plaques were used the pore size distribution could not be controlled, although it is known to play an important part in determining the electrical output, especially at high rates of discharge. Strength of sinter is of great importance for the successful use of the thermal method of impregnation, because of the oxidation of plaques during both the immersion and thermal decomposition steps. It was observed that plates which were loaded to greater than 0.30 AH cm.$^{-3}$ with active material disintegrated on cycling. It is necessary, therefore, to reduce the concentration of the immersion solution if more than one impregnation cycle is to be used.

The thick (0.080 in.) plaques used in this study developed blisters after one impregnation cycle, but it must be recorded that they appeared to be more poorly sintered than the thin (0.025 in.) plaques with which this difficulty was not encountered. In general the capacity per cubic centimeter of the thick plates was slightly lower than that of the thin plates produced under the same conditions.

The polarization step of the vacuum impregnation method has been found in this laboratory to precipitate the $Ni(OH)_2$ near the outside surface of thick plaques (1) leaving the center of the plaques nearly empty, and several

electrical cycles are necessary to bring the plate up to full capacity at higher rates. The present method of thermal decomposition seems to effect a more even gross distribution initially. However, there may be differences in distribution on the walls of individual pores owing to unknown variables in the processing; certain results which will now be discussed seem to substantiate this.

Addition Agents

The low rate capacity of the plaques produced was sometimes much lower than the theoretical. At temperatures above the optimum (Fig. 1), part of the reaction has probably gone to completion, forming NiO which is not available for reaction. Plates made at low temperatures may contain material which is in poor physical contact with the sinter. In plates made near the optimum, some plates had a low percentage utilization (real capacity/theoretical capacity), probably owing to a high resistance in the plate. It was found that this condition could be remedied by adding LiOH to the electrolyte in the test cell. After cycling in LiOH electrolyte the plate retained full capacity for more than 10 test cycles after being replaced in KOH electrolyte. Adding LiOH ($\sim$1 molar) directly to the conversion solution resulted in plates of slightly better performance, especially at high rate.

Some experiments were done in which foreign ions, which might be expected to alter the ionic conductivity of the solid oxides, were added to the immersion solution in portions varying from 0.002–2 mole %. The addition of lithium, silver, and cobalt ions generally gave plates whose performance fell within the limits of experimental error of plates made by the standard method but ensured close to 100% utilization at low rates. About 0.02 mole % silver ion in the immersion solution improved the high rate performance about 10%. High concentrations of cobalt ion (2%) and all concentrations of aluminum ion decreased the % utilization of active material at both high and low rates. These results are in qualitative agreement with other work on the conductivity of $Ni(OH)_2$ containing foreign ions (5).

The addition of foreign ions increased slightly the voltage of the plates on discharge at low rates. In general, large additions increased shedding of active material from the plate.

An Optimum Single Impregnation Process

In summary, it has been found that under the following conditions a plate of real capacity up to 0.26 AH $cm.^{-3}$ at 20 hour rate can be made if the precautions already discussed are observed.

Preparation of plaque:	Degrease in warm acetone.
Immersion:	10 min. vacuum at 115° C., rapid transfer to oven.
Thermal decomposition:	in air at 230° C. for 1 hour, rapid transfer to hot aqueous KOH.
Conversion:	in KOH_{aq} at 75–85° C., for 60 minutes (if not stirred).
Washing and drying:	see Table I.

Fig. 2 shows behavior of commercial plates prepared by the electrolytic method as compared with that of singly-impregnated plates prepared by the thermal decomposition method. Capacity per unit volume is plotted against log current density (for convenience) for plates 0.025 inch thick. The plates prepared by the new method behave electrically as well as did commercial plates under test conditions.

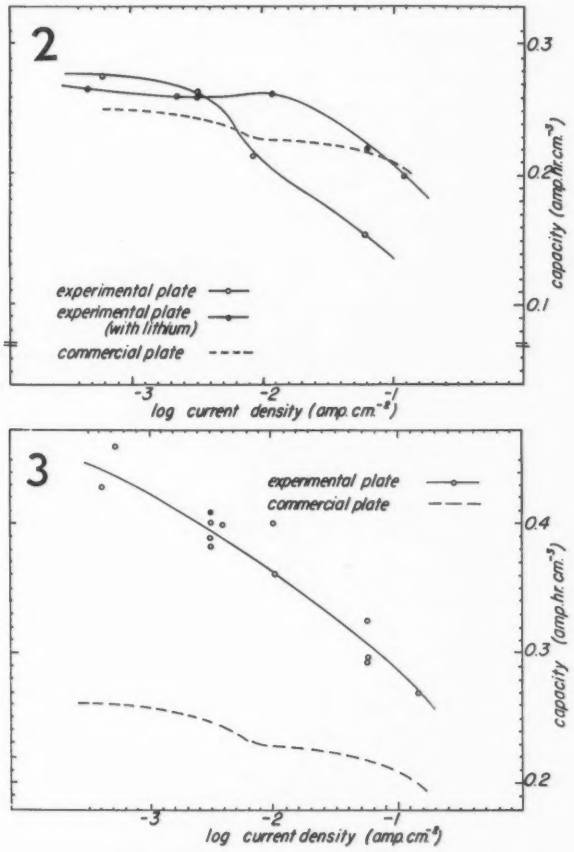

FIG. 2. Performance of experimental plates.
FIG. 3. Performance of a doubly impregnated experimental plate.

Double Impregnation

It has been shown that it is possible to produce in one impregnation a plate as good as the standard commercial plate which requires four impregnations. A series of plaques were given two impregnations by the thermal decomposition method. The real capacities (3 hour rate) were roughly double those of plaques

impregnated only once under the same conditions. Plaques which were given two cycles with 2-hour immersion at 95° C. had theoretical capacities about 0.40 AH cm.$^{-3}$ Blistering occurred during the processing, and the plate started to disintegrate after three cycles. Plates doubly impregnated by vacuum immersion at 95° C. had capacities as high as 0.35 AH cm.$^{-3}$ and were physically sound after processing, but still showed some tendency to disintegrate after 40 cycles. It seems probable that physically strong plaques can be impregnated to about 0.30 AH cm.$^{-3}$ and remain structurally sound during prolonged cycling. However, the much higher capacities available by double impregnation may be advantageous for applications requiring only a limited cycle life. The advantage with respect to capacity alone offered by double impregnation is clearly shown in Fig. 3.

SUMMARY

1. A new method of impregnating electrically active $Ni(OH)_2$ into the pores of sintered nickel plaques has been worked out. With a single impregnation cycle by this method, plates of capacity as high as that of commercial plates made by four standard cycles can be made.

2. Doubly impregnated plates, made by variations of this method, give strong plates with much higher capacity than the standard commercial plates, and whose electrical output even up to currents of 1 amp. in.$^{-2}$ exceeds that of commercial plates.

3. Some preliminary studies and discussions on the probable mechanism of the thermal decomposition are presented. The thermal decomposition proceeds toward an intermediate, tentatively called $Ni(OH)NO_3$, thence to electrolytically-inactive black NiO. If the decomposition is stopped at or before the intermediate stage, the material can then be converted to active hydroxides by dipping in aqueous KOH.

ACKNOWLEDGMENTS

The authors wish to acknowledge the contributions of Mr. J. Goodings and Mr. P. C. Clapp for technical assistance, and of Dr. I. H. S. Henderson of this Laboratory for important suggestions concerning the addition of foreign ions. The permission to publish granted by the Defence Research Board is appreciated.

REFERENCES

1. Casey, E. J., Bourgault, P. L., and Lake, P. E. Can. J. Technol. 34: 95. 1956.
2. Fleischer, A. Trans. Electrochem. Soc. 94: 289. 1948.
3. Kano, Y. and Wakayama, M. Japan Patent No. 175,733. 1948. (To Nippon Electric Co.)
4. Koren, H. W. and Baumstark, G. U.S. Patent No. 2,696,515. 1954. (To Sonotone Corporation)
5. Tichenor, R. L. Ind. Eng. Chem. 44: 973. 1952.

NEUTRON MOISTURE METER FOR CONCRETE[1]

By J. Pawliw and J. W. T. Spinks

ABSTRACT

Neutrons emitted by a Ra–Be neutron source are slowed down by the moisture in moist concrete. The resulting slow neutrons may be measured using a BF_3 chamber. These observations have led to the construction of a portable moisture meter which will give a rapid non-destructive measurement of the total moisture content of a concrete member.

INTRODUCTION

The determination of water content in concrete is of considerable importance with reference to predicting the durability of a concrete structure. A number of methods have been tried (12, 14), but all seem to suffer from some disadvantage. For example, the generally accepted procedure of drying and weighing a sample has the drawback that it involves the destruction of a portion of the structural member.

A neutron diffusion method of moisture detection has proved successful with soils (2, 3, 4, 9, 10, 13, 15, 16, 17), and it was thought that a modification of the method might lead to a procedure for the non-destructive determination of water in concrete.

Neutron Soil Moisture Meter

In the neutron method, as applied to soils, fast neutrons emitted by a neutron source are scattered by the atoms in the soil, thereby losing their energy and becoming slow neutrons (apart from loss by capture). The slow neutrons are then measured by means of a slow neutron detector such as an indium foil or a BF_3 chamber. The fractional loss in energy when a neutron collides with an atom is at a maximum for hydrogen (1, 7), and thus soils with a high moisture content are particularly effective in slowing down neutrons. The activity induced in a slow neutron detector is correspondingly high and is, in fact, proportional to the moisture content of the soil when standard conditions of neutron irradiation are adopted. It can be shown theoretically that the distribution of slow neutrons about a point source of fast neutrons in an infinite medium is a function of the ratio of the slowing down length to the diffusion length (18). The slowing down length is defined as the average distance a neutron must travel in a medium before it is slowed down to thermal velocity. It is relatively small for hydrogen in comparison with other common elements in soils. The diffusion length is one-sixth the average distance from point of origin to point of capture of the neutron. It does not vary with changing moisture content as strongly as does the slowing down length. The net effect is that if a slow neutron detector is placed near a

[1]*Manuscript received November 2, 1956.*
Contribution from the Department of Chemistry, University of Saskatchewan, Saskatoon, Sask.

source of fast neutrons in soil, the activity will be largely a function of the hydrogen (or moisture) content of the soil.

Application to Cement and Concrete

Considerations similar to the foregoing apply to moist concrete. The main chemical constituents of cement and concrete are a series of compounds comprising the elements calcium, aluminum, silicon, magnesium, iron, oxygen, and to a lesser extent, sodium, potassium, sulphur, and hydrogen. The neutron thermalizing effects of these elements are given in Table I. From this data it

TABLE I

PROPERTIES OF NUCLEI

Element	Atom % in dry cement	Collisions required for thermalization of 1 Mev., neutrons	Cross section (barns) for thermal neutrons	
			Capture	Scattering
Fe	0.9	515	2.4	11.3
K		362	1.9	2.0
Ca	28.7	370	0.4	3.3
S	0.3	289	0.5	1.2
Si	8.9	261	0.1	2.2
Al	3.7	252	0.2	1.3
Mg	1.5	228	0.06	3.9
Na		215	0.5	3.3
O	56	114	10^{-4}	3.7
H		18	0.3	20

is quite apparent that the neutron thermalizing effect of cement can be assumed to be due entirely to its hydrogen content and thus to the amount of water that it contains. Two limitations, however, arise in that the hydrogen content of cement is not wholly due to its water content. Hydrated cement is known to contain some $Ca(OH)_2$, but the discrepancy caused in this manner is believed to be slight. The second limitation arises from the fact that the neutron method will not differentiate between free water and water chemically bound in the form of hydration compounds. A further limitation would arise if the cement or concrete contained a substance, such as boron, with a high neutron capture cross section. Fortunately this occurrence is likely to be rare except in the case of concretes especially designed to absorb neutrons.

EXPERIMENTAL

Neutron Source

A 50 Mc. Ra–Be neutron source, obtained from the Atomic Energy of Canada Limited, was used as source of fast neutrons. When not in use it was kept in a lead container of about 80 lb. weight.

Thermal Neutron Detector

The detector used was a BP14-B type BF_3 tube, constructed and filled by the Counter Development Section of the Atomic Energy of Canada Limited

(5, 6). It has a copper cathode 0.75 in. in diameter, 0.05 in. thick, with a sensitive length of 4 in. The counter tube is filled with B^{10} enriched BF_3 to a pressure of 60 cm. mercury. Since the capture cross section for B^{10} is 3990 barns for thermal neutrons and less than 1 barn for 0.1 Mev. neutrons, such a tube forms an excellent detector for the purpose in hand (1).

Preliminary Laboratory Tests

Preliminary tests were made with a soil moisture meter (10) which had been modified by replacing the indium detector foils by a BF_3 counter. The required voltage was obtained from an 1800 volt battery pack and the pulses were recorded with a portable rate meter (Nuclear Instruments model 2610A) after amplification by a two stage vacuum tube preamplifier (13). In some experiments, pulses were recorded with a portable scaler (Berkely portable scaler, model 2080) or with a bench scaler (Nuclear Instruments, model 162). The neutron source was held by a clamp as close as possible to the BF_3 counter since both theoretical considerations and experimental observations indicate that maximum sensitivity of the soil moisture meter is obtained when the fast neutron source is as close as possible to the slow neutron detector (17). Furthermore, the effect on the counting rate of neutrons slowed down by collisions with nuclei other than hydrogen can be eliminated by placing the slow neutron counter as near as possible to the source of fast neutrons. In this position the counting rate is almost entirely a function of the amount of hydrogen in the surrounding medium (9).

The sensitivity of the modified meter was compared to the sensitivity of the original apparatus in an experiment in which the back diffusion of thermal neutrons was measured at different points within a composite paraffin wax–sand block (15), as illustrated in Fig. 1*a* and 1*b*. The relative thermal neutron

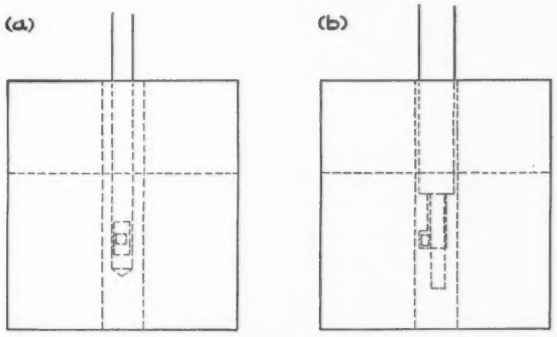

FIG. 1*a*. Schematic arrangement of sand, wax, and indium detector.
FIG. 1*b*. Schematic arrangement of sand, wax, and BF_3 counter.

flux at the different positions within the block, as determined by each instrument, is shown in Fig. 2. The BF_3 counter is evidently quite satisfactory. It has the added advantage that it gives a more or less instantaneous reading

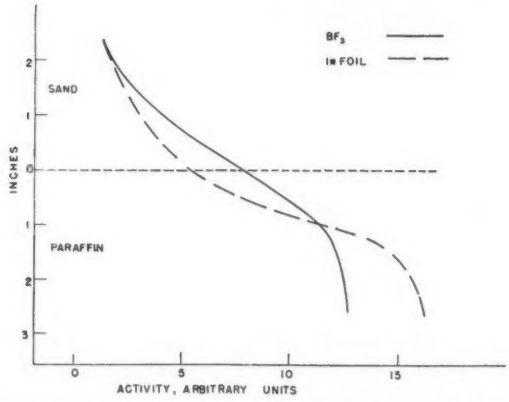

FIG. 2. Thermal neutron flux indicated by indium foil detector and BF_3 counter.

whereas with indium foils one has to wait for some minutes for the activation of the indium foils and then for a further period to measure the activity of the foils.

To indicate water content the soil moisture meter is placed in a hole in the soil. Thus the meter is almost completely surrounded by the neutron thermalizing material. The concrete moisture meter, on the other hand, will not be placed in a hole in the concrete member, but rather, it will be placed against the concrete surface. Consequently, for this geometry, the effective neutron thermalizing volume of a concrete member will be considerably less than it is for a soil body and the sensitivity will be correspondingly less.

As a means of counteracting this decrease in sensitivity a U-shaped neutron "reflector" was placed over the counter and source in such a manner as to reflect some of the neutrons, which would otherwise have escaped, into the concrete. To prevent appreciable neutron capture and thermalizing effect the reflector material should have a small capture section and a low neutron thermalizing capacity. Such a reflector would merely scatter the fast neutrons and increase the number of these neutrons entering the concrete. Furthermore, slow neutrons returning to the surface by back diffusion might also be directed towards the counter by scattering within the reflector.

In a further preliminary experiment the soil moisture meter was placed against the surface of a neutron thermalizing medium, and a number of steel reflectors of varying thicknesses were placed over the BF_3 counter, as shown in Fig. 3. The effect of a lead reflector was also investigated. The increases in slow neutron count caused by the different steel reflectors and by the lead reflector are shown graphically in Fig. 4. Fig. 4 indicates that a U-shaped neutron reflector will appreciably increase the sensitivity of the concrete moisture meter.

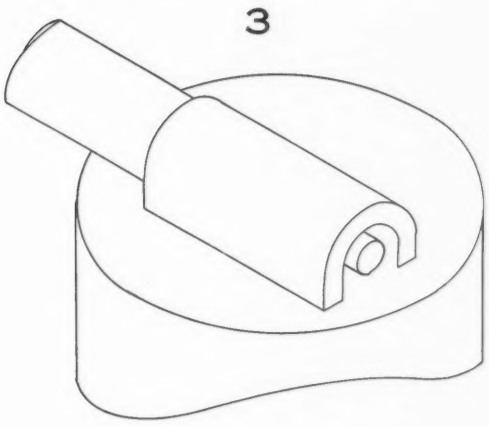

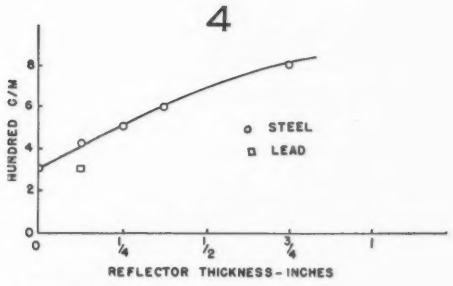

FIG. 3. Arrangement of steel reflector over BF_3 counter.
FIG. 4. Dependence of thermal neutron flux (as measured by BF_3 counter) on reflector thickness.

Design and Construction of Meter

The external structure of the meter was so designed as to enable an operator to handle the meter during short intervals of time without exposing himself to excessive radiations from the source. The end-to-end arrangement of the counter tube, the preamplifier, and the handle, as shown in Fig. 5, enables the operator to be at least 18 inches away from the source while handling the meter. As an additional safety precaution the meter was equipped with long connector cables. These cables permit the operator to be a distance of 12 feet from the source when operating the scaler.

A 1-in. thick U-shaped cast iron reflector was machined to fit over the BF_3 counter as shown in Fig. 6.*

A high gain four-stage amplifier was designed to receive the small BF_3

**The effect of a cast iron reflector was similar to that of the steel reflector.*

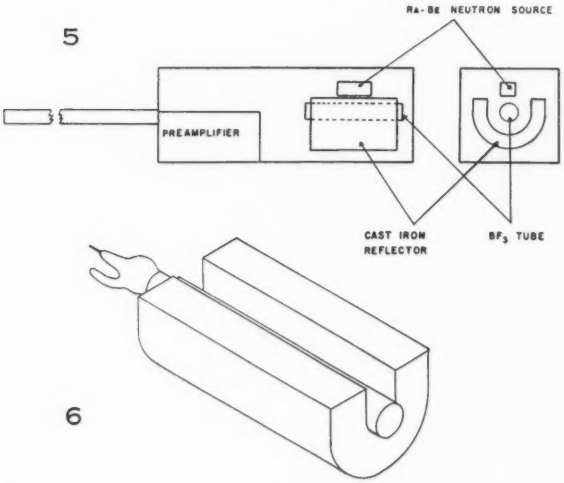

FIG. 5. Layout of neutron moisture meter for concrete.
FIG. 6. Cast iron reflector and BF_3 counter (scale 3/4 in. = 1 in.).

counter pulses and amplify them sufficiently to pass through the long connector cable and trip the scaling mechanism. This amplifier, henceforth referred to as the preamplifier, to distinguish it from any amplifying device within the scaler, is shown schematically in Fig. 7.

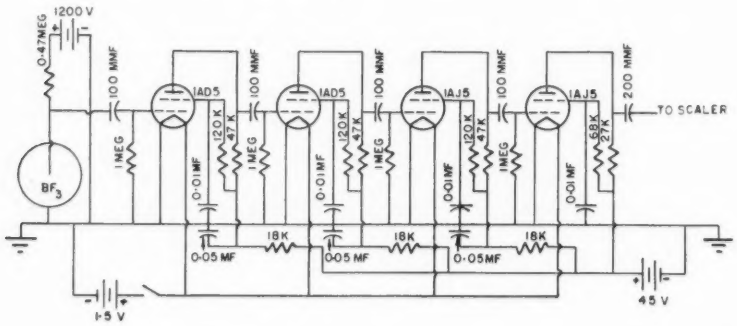

FIG. 7. Preamplifier.

To correct for fluctuations in the background count and slight variation in the counter and/or preamplifier voltage, a standard paraffin neutron thermalizer was designed and constructed (Fig. 8). This enabled the operator to compare all observations with the response from a constant neutron thermalizing medium.

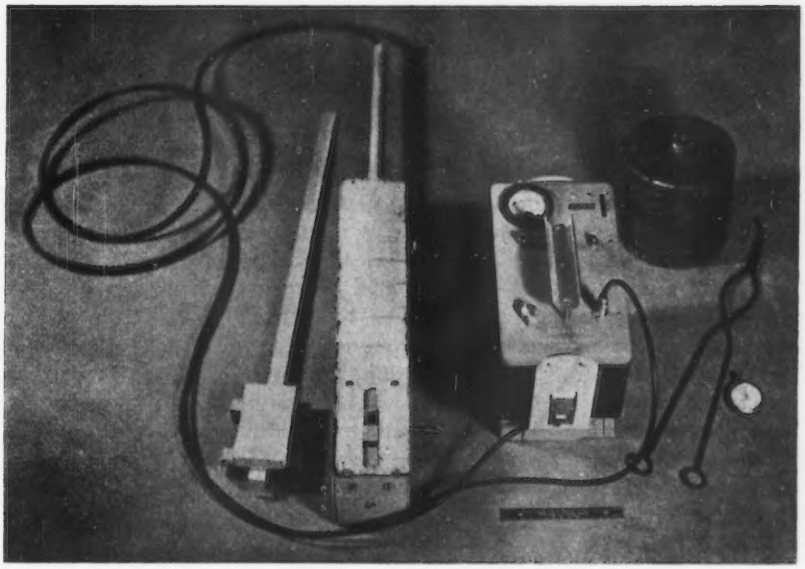

FIG. 8. Portable concrete moisture meter (paraffin neutron thermalizer to left).

All observations were recorded as the "relative thermal neutron count"

$$= \frac{\text{observed count} - \text{background count}}{\text{standard paraffin count} - \text{background count}}$$

where the background count and the standard paraffin count were determined immediately after the required observation was recorded.

The concrete moisture meter, adapted for field use, is shown in Fig. 8.

Preliminary Tests with Concrete Moisture Meter

(*a*) *Optimum operating voltage and preamplification.*—The BF_3 counter gas is ionized by gamma rays and by neutrons, the pulses created by the gamma rays being considerably smaller than the pulses created by the neutrons. The size of the pulses entering the scaling unit depends on the counter voltage and on the gain in the preamplifier and an optimum state of affairs would be one in which the neutron pulses would trip the scaling mechanism, but the gamma ray pulses would not. With the equipment at hand it was not found possible to eliminate the effect of gammas entirely and so preliminary experiments were done in which applied voltage and amplifier gain were varied and plateau curves drawn using a block of paraffin wax as neutron thermalizer. As a result, 1200 volts counter voltage and a preamplifier gain of approximately 10,000 were chosen as the best working combination for our equipment.

(*b*) *Effect of cast iron reflector.*—A simple laboratory experiment was per-

formed to test the effect of the cast iron reflector on the thermal neutron count of the concrete moisture meter. The reflector was removed and a series of observations were taken with the paraffin standard in place and with the standard removed. The effect of the cast iron reflector was to increase the thermal neutron count by a factor of 2.35 (11).

Calibration of Neutron Moisture Meter for Concrete

The neutron thermalizing effect of a material such as concrete is almost entirely dependent on its water content, or more specifically, on its hydrogen content. The density of the material has no marked influence on the back diffusion of thermal neutrons (3). The effective neutron thermalizing volume of a substance is dependent on the water content of the substance and it is therefore necessary to determine edge and depth effects. The investigation of these effects is facilitated by using synthetic mixtures of sand and sugar in the place of concrete blocks. Sugar may be regarded as 57.9% water and 42.1% carbon, and a mixture of sand and sugar, of any given concentration, has a corresponding equivalent water content. The neutron thermalizing effect of the mixture depends on this equivalent water content. A number of sand–sugar mixtures were prepared with the equivalent water content ranging from 0.135 to 0.334 g./cc.

Edge and depth effects were then investigated using cylindrical vessels, of various radii and depths, filled with the mixtures and with water. The vessels were made of tin sheet and did not themselves contribute appreciably to the neutron thermalization. Measurements were made with the neutron source at the center of the flat surface of the cylindrical vessel. Figs. 9 and 10 show graphically the effect of radius (and hence effective area of cross section) and depth of material on neutron thermalization for materials of different water content. Fig. 11 is a plot of data derived from Figs. 9 and 10. This plot indicates the minimum dimensions of the above materials which will enclose the whole of their effective neutron thermalizing volume. The plot of the asymptotic value of the relative thermal count versus water content, as derived from the sand–sugar experiments, is shown in Fig. 12. Figs. 11 and 12 would also be expected to apply quite closely to concrete. Using the data exhibited in Fig. 11 as a guide, two concrete cylinders were made, each with a diameter of 18 in. and depths of 8.3 and 8.75 in., respectively. Each cylinder consisted of three slices of equal thickness. This simplified the handling of the concrete specimens and made the removal of the water from the concrete somewhat more uniform.

Each concrete specimen was mixed from 23 lb. Portland cement, 74 lb. light weight aggregate, and 21 lb. water. After 48 hours the forms were removed and the concrete was placed in water for several days. These concrete cylinders were then used to calibrate the concrete moisture meter. The water was removed from the concrete by heating the concrete in an oven at 130° F. This drying process was carried out in a stepwise manner and after each drying period the concrete was weighed and a relative thermal neutron count was determined, using the concrete moisture meter. Finally, when most of the

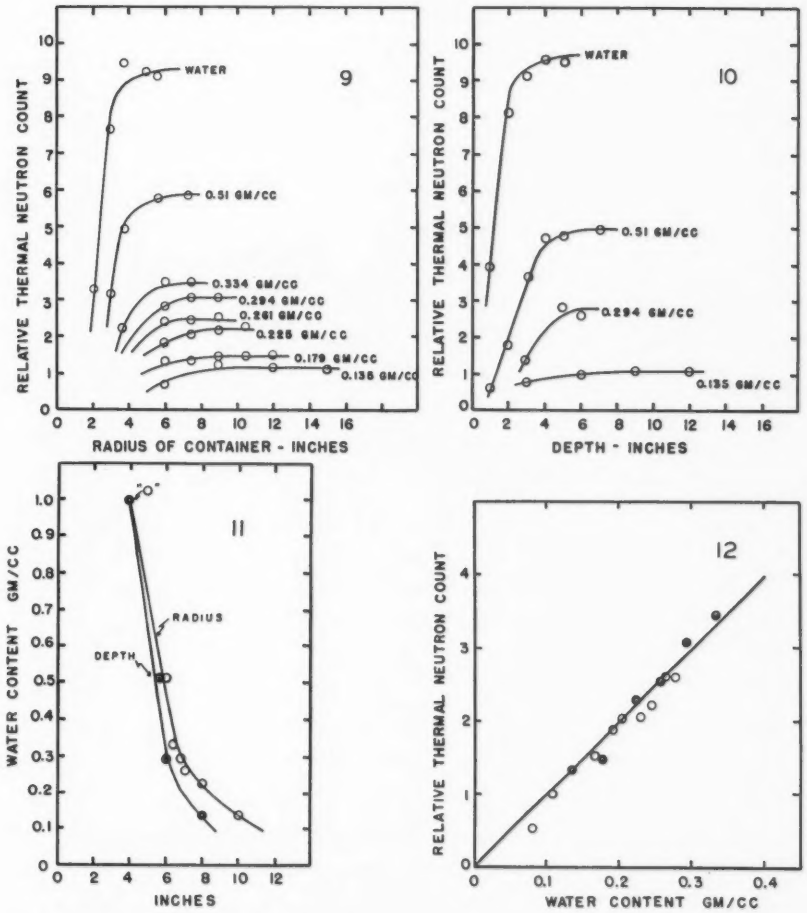

FIG. 9. Effect of radius of container on relative thermal neutron count for water and sand–sugar mixture of various equivalent water contents (depth: water, 5 in., other 9 in.).

FIG. 10. Effect of depth of container on relative thermal neutron counter for water and sand–sugar mixtures of various equivalent water contents (diameter of container: for water, 7½ in.; 0.51 g./cc. and 0.29 g./cc., 15 in.; 0.135 g./cc., 22 in.).

FIG. 11. Minimum desirable size (radius and depth) of concrete or similar material for moisture metering.

FIG. 12. Relative thermal neutron count versus water content: ○, concrete; ●, sand–sugar; — calculated curve.

water had been removed, the concrete cylinders were crushed with a jaw crusher and representative samples removed for further drying. In order to remove the total water, including the water chemically combined to form hydration products, these samples were heated to 1000° C. (12). The observations from this experiment are recorded in Table II, and are shown in Fig. 12 together

TABLE II

EFFECT OF WATER IN CONCRETE ON RELATIVE THERMAL NEUTRON COUNT

Wt. of concrete, lb.	Water content		Relative thermal neutron count
	lb./ft.^{3}	g./cc.	
Cylinder No. 1: (18 in. diam.; 8.3 in. depth)			
118.81	17.4	0.279	2.60
110.38	10.5	0.168	1.54
103.81	5.1	0.082	0.52
Cylinder No. 2: (18 in. diam.; 8.75 in. depth)			
112.50	16.6	0.266	2.62
111.06	15.5	0.248	2.23
109.94	14.6	0.234	2.07
107.88	13.0	0.208	2.03
106.94	12.2	0.195	1.88
100.06	6.9	0.111	1.00

with results from the sand–sugar experiment. This is effectively a calibration curve for our instrument.

A theoretical method of calibrating a neutron moisture meter for soils has been proposed (8). The relative thermal neutron count N^1, indicated by the moisture meter for a soil of water content W g./cc., is given by the equation $N^1 = N\,W\,F$, where N is the relative thermal neutron count indicated by the moisture meter for water, F is a factor given by the equation

$$[1]\quad F = \frac{e^{(-\bar{r}/L)W}\left\{1-\operatorname{erf}\left(\frac{\sqrt{\theta_0}}{L}-\frac{\bar{r}}{2\sqrt{\theta_0}}W\right)\right\}+e^{(\bar{r}/L)W}\left\{1-\operatorname{erf}\left(\frac{\sqrt{\theta_0}}{L}+\frac{\bar{r}}{2\sqrt{\theta_0}}W\right)\right\}}{e^{(-\bar{r}/L)}\left\{1-\operatorname{erf}\left(\frac{\sqrt{\theta_0}}{L}-\frac{\bar{r}}{2\sqrt{\theta_0}}\right)\right\}+e^{(\bar{r}/L)}\left\{1-\operatorname{erf}\left(\frac{\sqrt{\theta_0}}{L}+\frac{\bar{r}}{2\sqrt{\theta_0}}\right)\right\}},$$

$\sqrt{\theta_0}$ = slowing down length of neutrons in water (6.80 cm.),
L = diffusion length of neutrons in water, (2.88 cm.), and
$\bar{r}$ = distance between source and point where the thermal neutron flux is measured.

The value of $\bar{r}$ cannot be measured directly; it can, however, be calculated from experimental data obtained from a sample of known water content. In other words, knowing N^1, N, W, and F, a value for $\bar{r}$ can be found by trial and error to give the required F. $\bar{r}$ depends on the geometry of the instrument and is constant for different values of W.

This method was believed applicable to the concrete moisture meter. The value of $\bar{r}$ for the concrete moisture meter was found to be 3 cm. F remained very nearly constant for all values of W being considered. This made the theoretical calibration curve, calculated from equation [1], a straight line. This curve is plotted in Fig. 12, together with the experimental plots. There is obviously quite good agreement between theory and experiment.

CONCLUSION

The foregoing has indicated that it is quite feasible to construct a portable moisture meter which will give a rapid non-destructive measurement of the moisture content of a concrete member.* It is proposed in future models to replace the 50 Mc. Ra–Be source by one of 10 Mc., which would still give a satisfactory neutron count but would require less shielding. It is also proposed to use a BF_3 chamber with a smaller sensitive length, 2 in. instead of 4 in.

ACKNOWLEDGMENTS

We are grateful to the Division of Building Research of the National Research Council for financial assistance. Thanks are also extended to Mr. H. Busse and Professor B. Torchinsky, College of Engineering, University of Saskatchewan, for helpful suggestions.

REFERENCES

1. Baum, J. W. Neutron Dosimetry—A Review. The University of Rochester Atomic Energy Project. Rochester, N.Y. March, 1956.
2. Belcher, D. J., Herner, R. C., Cuykendell, T. R., and Sacks, H. S. ASTM Special Tech. Publ. No. 134. 10. 1952.
3. Brocard, J. Application of radioisotopes to non-destructive testing of materials. Intern. Assoc. of Testing and Research Lab. for Materials and Structures. Bull. No. 20. Dec., 1954.
4. Brocard, J. Rev. des matériaux. Numero du Cinquantenaire. No. 482–483. 142. 1955.
5. Flowers, B. H. Proportional neutron counters. A.E.C.L. No. 62. 1946.
6. Fowler, I. L. and Tunnicliffe, P. R. Rev. Sci. Instr. 21: 734–740. 1950.
7. Glasstone, S. Source book on atomic energy. D. Van Nostrand Company, Inc., New York. 1950.
8. Holmes, J. W. Australian J. Appl. Sci. No. 1. 45. 1956.
9. Knight, A. H. and Wright, T. W. Soil moisture determination by neutron scattering. Proc. of the Second Radioisotope Conf., Oxford. July, 1954.
10. Lane, D. A., Torchinsky, B. B., and Spinks, J. W. T. ASTM Special Tech. Publ. No. 154. 23. 1952.
11. Pawliw, J. M.Sc. Thesis, University of Saskatchewan, Saskatoon, Sask. 1956.
12. Powers, T. C. and Brownyard, T. L. Studies of the physical properties of hardened Portland cement paste. Research Labs. of the Portland Cement Assoc. Bull. No. 22. March, 1948.
13. Saskatchewan Research Council. 9th Ann. Rept. 22. 1955.
14. Spencer, R. W. Proc. Am. Concrete Inst. 34: 45. 1938.
15. Spinks, J. W. T. Can. Chem. Processing, 63. Oct., 1955.
16. Spinks, J. W. T., Lane, D. A., and Torchinsky, B. B. Can. J. Technol. 29: 371. 1951.
17. Stone, J. F., Kirkham, D., and Read, A. A. Soil Sci. Soc. Amer. Proc. 19: 419. 1955.
18. Wallace, P. R. Nucleonics, 4: 30. 1949.

**Care would have to be taken in interpreting the readings if the concrete member contained any appreciable amount of steel reinforcing or if the moisture distribution were non-uniform.*

VAPOR–LIQUID EQUILIBRIUM DATA FOR SYSTEM: *n*-OCTANE – PROPIONIC ACID, WITH SALT EFFECT[1]

By A. I. Johnson, D. M. Ward, and W. F. Furter

ABSTRACT

New isobaric vapor–liquid equilibrium data at one atmosphere pressure are reported for the binary system *n*-octane – propionic acid. These data are compared to those of a previous investigation in which a different type of apparatus was used.

The salt effect of saturated sodium propionate on the binary vapor–liquid equilibrium curve of the system *n*-octane – propionic acid is reported. The salt was found to enhance the relative volatility and alter the azeotropic composition of the binary system in the manner predicted.

INTRODUCTION

Vapor–Liquid Equilibrium Data

The vapor–liquid equilibrium relationships of the binary system *n*-octane – propionic acid at atmospheric pressure were originally established by Johnson, Furter, and Barry (1, 2) using a modification of the Colburn (3) type of recirculation still in their investigation. The purpose of the present work (5) was to check these data by using another variety of equilibrium still, to see if consistent data on the same system would be produced by two different types of still, and to increase the data available on this binary system.

For the present investigation, a slightly modified version of the improved Othmer still (4) was selected. The Othmer still continues to be chosen over various other designs by the majority of investigators because of its simplicity of construction and operation and because of its proved reliability over a wide variety of systems.

Salt Effect

Distillation often affords the most suitable method of separating a binary mixture. In the design of distillation equipment, the vapor–liquid equilibrium relationships between the components to be separated are of prime importance. Consequently any factors permitting the altering of relative volatility or the shifting of azeotropic compositions will greatly affect design. Salt effect, or the presence of a dissolved solid third component in the downflowing liquid stream within the column, is such a factor.

When a salt is dissolved in a pure liquid, the general effect is a lowering of the vapor pressure of the liquid and an elevation of its boiling point. The extent of this effect is a function of the quantity of solid dissolved. Hence in a binary system, a solid which is more soluble in the less volatile, higher-boiling component than in the other would be expected to depress the vapor pressure or volatility of the less volatile component by an amount greater than that of

[1]*Manuscript received October 29, 1956.*
Contribution from the Department of Chemical Engineering, University of Toronto, Toronto, Ontario.

the more. In other words the net effect would be an increase in the relative volatility or ease of separation of the binary system. The purpose of the second portion of this work was to investigate the effect of such a solid on the vapor–liquid equilibrium relationships of the system under study.

The system *n*-octane – propionic acid was chosen to check the data of Johnson, Furter, and Barry and, as well, for the following reasons. It has an azeotrope located close enough to the central portion of the composition range to be suitable for a study of its shift due to salt effect. The system is not excessively volatile. It is stable. Samples may be readily and simply analyzed for composition by acid–base titration. Relative volatility is low enough to show clearly changes caused by salt effect. Since *n*-octane is non-polar and propionic acid is polar, possibilities are good that salts could be found that would have solubilities markedly different in one component of the binary as opposed to the other. Sodium propionate was chosen as the salt because of its high solubility in propionic acid as opposed to its negligible solubility in *n*-octane. It was also chosen because of its stability against decomposition and chemical reaction when dissolved in the binary system.

EXPERIMENTAL METHOD AND RESULTS

Reagent grade propionic acid, *n*-octane, and sodium propionate were obtained from Matheson, Coleman, and Bell Inc., of New Jersey.

The improved recirculation still design of Othmer was modified by lengthening the flask neck in order to better protect against entrainment. A double layer of magnesia–asbestos lagging was used to cover the neck and upper portion of the pot. A chromium wire winding was included between the two layers of lagging to create a vapor superheat of from one to two degrees above the temperature of the boiling liquid, in order to prevent condensation within the boiling chamber. The flask was heated with a glass-col electric heater. Both heaters were controlled by rheostats. Standard-taper thermometers were mounted in the still neck and pot to measure the temperatures of the vapor and boiling liquid. The thermometer immersed in the boiling liquid was calibrated by consecutively boiling several pure liquid substances in the pot. A calibration chart was drawn, and from it the boiling point data were corrected. The corrected boiling point data are reported in the results section.

The still was tested for entrainment by dissolving sodium sulphate to saturation in a boiling binary mixture and testing samples from the distillate chamber for precipitation with a solution of barium nitrate. The test was negative for as high boiling rates as possible from the glass-col heater. Hence entrainment was rejected as a possible source of error.

The rate of approach to steady state was studied by first charging the still with a binary mixture in which the liquid composition differed as markedly as possible from the equilibrium vapor composition, and then withdrawing exceedingly small samples from the pot and residue chambers and reading the pot thermometer at regular intervals of time. At the boiling rate used in

TABLE I

BINARY VAPOR–LIQUID EQUILIBRIUM DATA FOR SYSTEM: *n*-OCTANE – PROPIONIC ACID
(Pressure is 750±10 mm.)

Temperature, °C.	Mole % *n*-octane		Relative volatility
	In liquid (x)	In vapor (y)	
124.8	96.7	91.8	0.38
123.7	93.8	87.8	0.48
122.9	88.8	82.7	0.60
122.0	76.6	73.1	0.83
121.8	70.1	69.0	0.95
119.8	64.9	66.0	1.08
121.4	59.5	64.8	1.25
121.9	46.1	56.6	1.55
122.6	36.1	51.2	1.85
—	25.8	44.7	2.33
—	20.5	40.7	2.66
129.2	13.5	33.7	3.25
133.2	8.2	23.4	3.42
136.8	5.1	12.0	2.54

the investigation, essential steady state was reached in 15 minutes. Temperature steady state coincided with composition steady state. During subsequent runs the still was allowed to operate for approximately 30 minutes before sampling to ensure that steady state conditions were closely approached.

Tests made at 5°, 10°, and 15° vapor superheat using charges of the same composition indicated no variation in vapor composition. It was concluded that although negligible total vaporization of splashed droplets did occur even at superheats as high as 15°, superheat should be kept at the minimum value necessary to just prevent premature condensation.

The mode of operation was similar to that described by Othmer. After allowing sufficient time for steady state to be attained, small samples from the pot and condensate chambers were quickly withdrawn into cooled weighing bottles, immediately stoppered, cooled to room temperature, and weighed. A 1 ml. sample was pipetted from each bottle into distilled water and titrated with standardized base. The remaining droplet in the pipette was returned to the weighing bottle, which was then reweighed. Per-cent-by-weight composition data were obtained directly by the above method, and were converted to a mole % basis. The results appear in Table I and Fig. 1.

For studying the effect of saturated sodium propionate on the binary vapor–liquid equilibrium curve, the method of analysis was similar to the above with the following change. Salt was added through a port in the side of the flask until saturation was attained. At steady state, a sample of solution of exactly 1 ml. size was pipetted from the pot into distilled water and titrated. An additional 1 ml. sample was pipetted into a tared weighing bottle, and was evaporated to dryness and finally to constant weight. From the difference in weights, the binary equilibrium pot compositions were calculated on a salt-

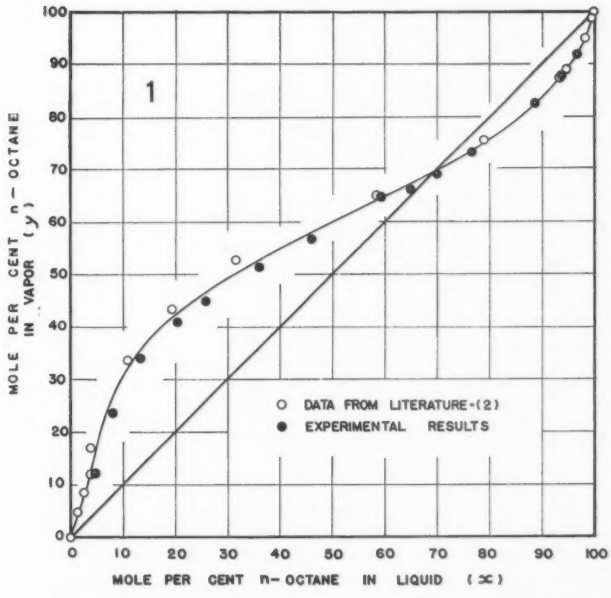
1
MOLE PER CENT n-OCTANE IN VAPOR (y)
MOLE PER CENT n-OCTANE IN LIQUID (x)
DATA FROM LITERATURE-(2)
EXPERIMENTAL RESULTS
0
10
20
30
40
50
60
70
80
90
100

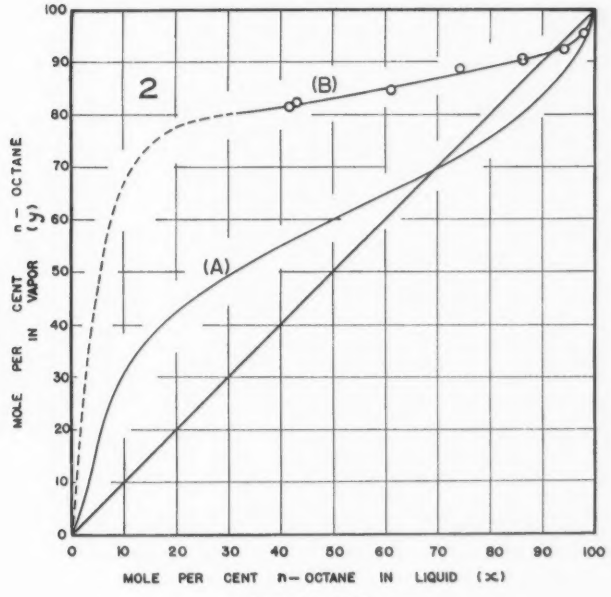
2
(A)
(B)
MOLE PER CENT n-OCTANE IN VAPOR (y)
MOLE PER CENT n-OCTANE IN LIQUID (x)
0
10
20
30
40
50
60
70
80
90
100

FIGS. 1 and 2.

free basis. Vapor–condensate samples were analyzed as before. The results appear in Table II and Fig. 2.

TABLE II

BINARY VAPOR–LIQUID EQUILIBRIUM DATA FOR SYSTEM: *n*-OCTANE – PROPIONIC ACID SATURATED WITH SODIUM PROPIONATE

(Pressure is 750±10 mm.)

Temperature, °C.	Mole % *n*-octane (salt-free basis)		Relative volatility
	In liquid (x)	In vapor (y)	
124.4	98.1	95.3	0.39
124.0	94.3	92.1	0.70
124.7	86.5	90.1	1.42
124.7	86.4	90.5	1.50
—	74.4	88.5	2.65
125.2	61.5	84.4	3.39
127.0	43.4	82.2	6.02
127.2	42.1	81.4	6.02

DISCUSSION

It is concluded that the slight discrepancies between the results of the present investigation and those of Johnson, Furter, and Barry are most likely due to inherent factors in the type of equilibrium still used. It is to be noted that the Colburn still was designed to eliminate certain sources of error in the Othmer design, such as the tendency of the lower-boiling condensate returning to the pot to flash on contact with the higher-boiling pot liquid rather than to mix well with it.

The saturated salt $x-y$ curve could not be completed using the techniques described. Difficulties were encountered in withdrawing salt solution samples from the pot by pipette at *n*-octane concentrations of less than 40 mole % owing to salt precipitation. Hence the remainder of the curve was estimated, and is shown as a dotted line in Fig. 2. Despite this, the effect of the salt is clearly evident. Sodium propionate is very soluble in the higher-boiling less volatile propionic acid while being almost insoluble in the lower-boiling more volatile *n*-octane. As predicted, the salt greatly enhanced the relative volatility of the system. In fact, of the more reliable salt effect data reported in the literature, the improvement factor reported for this system is especially large. An accompanying result of this salt effect was a shift in azeotropic composition from 67 to 92 mole % *n*-octane. The advantages of such an effect in distillation are apparent.

REFERENCES

1. FURTER, W. F. B.A.Sc. Thesis, Chemical Engineering Dept., University of Toronto, Toronto, Ontario. 1954.
2. JOHNSON, A. I., FURTER, W. F., and BARRY, T. W. Can. J. Technol. 32: 179. 1954.
3. JONES, C. A., SCHOENBORN, E. M., and COLBURN, A. P. Ind. Eng. Chem. 34: 693. 1942.
4. OTHMER, D. F. Ind. Eng. Chem., Anal. Ed. 20: 763. 1948.
5. WARD, D. M. B.A.Sc. Thesis, Chemical Engineering Dept., University of Toronto, Toronto, Ontario. 1956.

NOTES

MICROWAVE REFRACTOMETER CAVITY DESIGN

By Albert W. Adey

The microwave refractometer has become a valuable aid in tropospheric radio propagation research (1, 2).

The operation of the instrument involves the comparison of the resonant frequency of a sealed reference cavity with that of a cavity exposed to the atmosphere and ventilated by cutting away part of the end plate area.

One of the limiting factors in the use of the refractometer has appeared to be the long flushing time of the ventilated cavity. This is due to the small part (20–30%) of the end area cut away.

As part of a program of refractometer development in this laboratory it has been found that as much as 67% of the end area could be cut away without seriously affecting the cavity Q. The figure shows the cavity being used. It operates in the TE_{011} mode at a frequency of 9100 Mc./sec. An annular ring in the region of high circumferential current density essentially forms the end plate. With a barrel formed of invar, end plates formed of brass, and all the inner surfaces silverplated, a loaded Q of 16,000 has been achieved with 0.250 inch coupling holes. This value of Q could undoubtedly be exceeded with better surface treatment.

Cutting away the end area resulted in a decrease of the resonant frequency of 200 Mc./sec. This necessitated shortening the barrel. Because of feed difficulties due to this shortening, it was not possible to increase the ventilation further with this barrel design and also obtain a practical, temperature-compensated cavity.

For purposes of temperature compensation it is necessary to know the frequency sensitivity of the length of the projection of the ends into the cavity. For the 67% ends this has been found to be only 90% of that for the solid ends, necessitating the use of a longer projection.

Laboratory blower tests on this cavity have indicated a reduction of the recovery time by a factor of the order of 10.

It is apparent that the cavity design discussed so far is not omnidirectional in azimuth. Thus, for a fixed installation, some directivity effect results from its use. As a preliminary step toward developing an omnidirectional cavity a TE_{013} design has been attempted. Coupling is by wave guide at the ends, the coupling holes being cut at 48% of the radius from the center. This design permits the cutting of two sets of slots or holes around the periphery of the barrel in the regions of weak electric field.

Effective suppression of the unwanted TM_{212} mode has been achieved by (*a*) a proper choice of the cavity dimensions, (*b*) leaving a narrow gap between

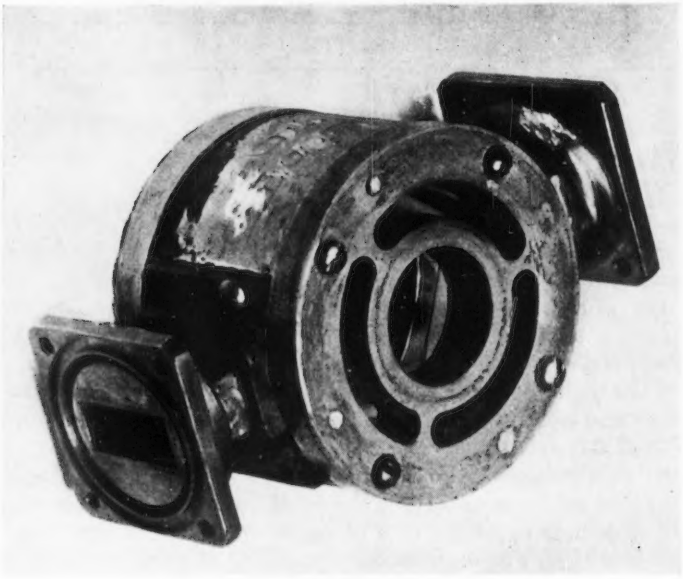

FIG. 1.

the inner surface of the ends and the barrel to impede the flow of radial currents, and (*c*) orienting the input and output wave guides at 45° to each other. A mode separation of 100 Mc./sec. has not been difficult to obtain. This is ample, since the refractometer is a narrow band device (approximately 5 Mc./sec.). Further work on this design is planned.

With regard to the reference cavity it may be of interest to note that it has been sealed by forming around it, by dipping, a closely-fitting sheath of Latex Ch 235* approximately 1/16 inch thick. Sealing of the Latex to the metal feed guides and the projection into which the tuning micrometer fits has been achieved by first coating the cleaned metal parts with Dupont Cement No. 1084. The cavity can thus be opened up easily and cleanly, should the necessity arise, merely by slicing open the Latex and peeling it off. The micrometer plunger used for tuning the cavity runs inside a thin walled polystyrene tube which has been cemented to the cavity end plate with Glyptal† cement. The entire micrometer assembly can thus be removed without destroying the cavity seal. This technique of sealing the cavity plunger seems to have originated with Crain, of the University of Texas. It has been found, however, that polystyrene seems to cement more readily than glass or quartz, which were used previously where a better temperature behavior was necessary.

The assistance of S. E. Forshaw, who made the cavity measurements,

**Manufactured by General Latex and Chemicals, Ltd.*
†Manufactured by General Electric Co., Ltd.

of W. J. Edwards of the Canadian Defence Research Board Chemical Laboratory, in the sealing of the reference cavity, and of Dr. G. Miller of the National Research Council, for the loan of a *Q* meter, is acknowledged.

This work was carried out under Defence Research Board Project No. PCC D–48–28–01–03.

1. Birnbaum, G. Rev. Sci. Instr. 21: 169. 1950.
2. Crain, C. M. Rev. Sci. Instr. 21: 456. 1950.

Received October 23, 1956.
Defence Research Telecommunications Establishment,
Radio Physics Laboratory,
Defence Research Board,
Shirley Bay,
Ottawa, Ontario.

ELECTRODELESS DISCHARGE LAMP EXCITER[1]

By D. S. Smith

An inexpensive oscillator, shown in the accompanying photographs and diagram (Fig. 1), has been found very convenient and effective for excitation of small electrodeless discharge lamps at 50 to 250 Mc./s.

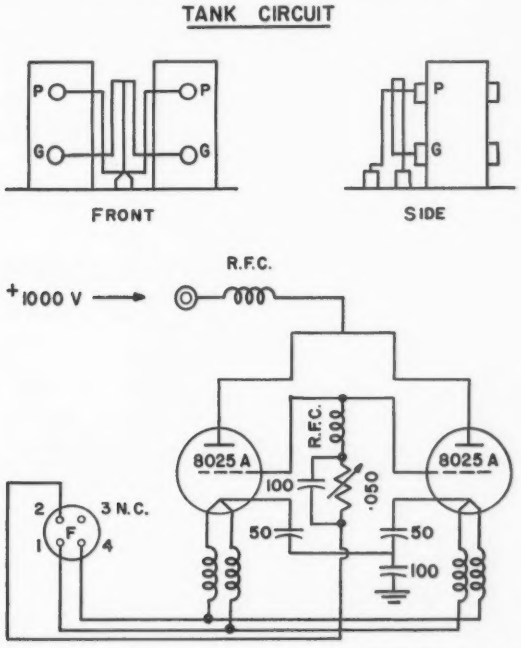

Fig. 1. Tank circuit. All resistances in megohms. All capacitances in micromicrofarads. R.F.C. to be wound on 1.0 M–2 watt resistor with No. 24 enamelled solid copper wire. Fil. chokes = No. 20 enamelled solid copper wire.

[1]*Issued as N.R.C. No. 4188.*

The Hg 198 lamp shown in Figs. 2 and 3 is contained in a water-cooling jacket, one end of the lamp protruding about ½ inch from the jacket. The lamp should not touch any of the metal parts of the oscillator as local blackening may occur.

The 50,000 ohm variable resistance in the grid circuit is adjusted for about 75 ma. plate current with a lamp glowing (i.e., under load), the resistance in the grid circuit is measured, and a 10-watt resistor near the measured value

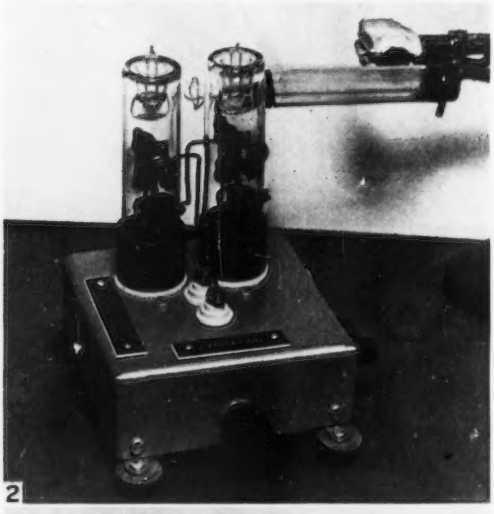

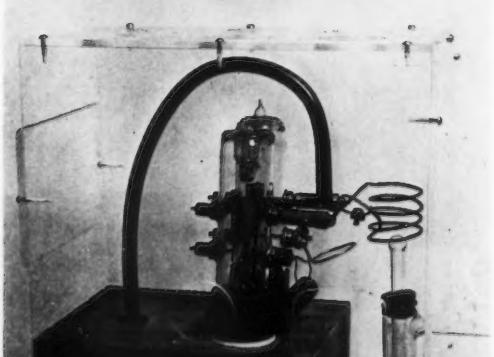

FIGS. 2 and 3.

is permanently wired in its place. The power coupled can be decreased by moving the lamp away or by reducing the plate voltage with a Variac. A grid current meter is connected between No. 2 connection and the filament supply center tap; this current should not be permitted to exceed 25 ma.

The coil dimensions are not critical. The two "hair-pin" coil assembly of Fig. 2 produces about 250 Mc./s. while the more conventional coil assembly of Fig. 3 resonates near 150 Mc./s. This frequency can be lowered by putting capacitance across the plate coil (from plate to plate). The coupling can be very loose between the plate and grid tanks. The coils should be hard-soldered to their connectors.

It is recommended that the 8025–A's be mounted upright and the circuit be made as symmetric as possible. The tube plates can be run dull red hot if forced-air cooling is provided.

If radiation from the unit affects nearby equipment it will usually be found sufficient to enclose the unit in a sheet-metal box with holes for forced-air cooling and for access to the lamp.

Received November 6, 1956.
Division of Applied Physics,
National Research Council,
Ottawa, Canada.

A NOTE ON THERMODYNAMIC CONSISTENCY TESTS OF BINARY VAPOR–LIQUID EQUILIBRIUM DATA

By Benjamin C.-Y. Lu

It is noted that when vapor–liquid equilibrium data are reported in the literature, their thermodynamic consistency has been usually checked by the authors in order to support their accuracy. The usual test methods employed for binary vapor–liquid equilibrium data are mainly as follows:

1. Logarithm plot of the activity coefficients vs. the liquid composition with the condition that the Gibbs-Duhem relationship be satisfied,
2. The Redlich-Kister relationship (6, 8) or its modified forms (2, 10).

Probably it is because the relationship between these methods has not been presented completely that unnecessary and wasteful efforts have been exerted in the testing of data (4, 5, 7, 11).

Several examples are chosen here for illustration. It should be mentioned, however, that the experimental measurements obtained by these investigators may be excellent. The discussion of this note is limited to the procedures employed, in these examples, for the testing of the data. The validity of these test methods is considered to be beyond the scope of this note and hence will not be discussed.

Hanson *et al.* (5) have correlated their binary vapor–liquid equilibrium data for the system ethylene–ethane by means of the five-suffix equation

$$[1a] \quad \log \gamma_1 = A(4x_1^3x_2 - 4x_1^4x_2) + B(6x_1^2x_2^2 - 8x_1^3x_2^2) + C(4x_1x_2^3 - 8x_1^2x_2^3) + D(x_2^4 - 4x_1x_2^4),$$

$$[1b] \quad \log \gamma_2 = A(x_1^4 - 4x_1^4x_2) + B(4x_1^3x_2 - 8x_1^3x_2^2) + C(6x_1^2x_2^2 - 8x_1^2x_2^3) + D(4x_1x_2^3 - 4x_1x_2^4).$$

This equation obeys the Gibbs-Duhem relationship and was obtained from generalized expressions developed by Benedict *et al.* (1). Hanson *et al.* (5) first adjusted the activity coefficients of their data by means of the Redlich-Kister relationship (8) and then substituted these activity coefficients into Equation [1] to calculate the four constants. Using these constants, values of the activity coefficients at 0.1 mole fraction intervals in x were calculated and tested again with the Redlich-Kister relationship. This last procedure would be necessary only if the Redlich-Kister relationship and Equation [1] were two independent test methods.

Otsuki and Williams (7) have employed the van Laar equation to fit the vapor–liquid equilibrium data for the binary system ethanol–water at various total pressures. Although close agreements between the calculated values and the experimental values for the activity coefficient have been obtained using the van Laar equation, they have tested the thermodynamic consistency of their data by the method of Redlich and Kister. Knowing that the temperature effect was negligible in the Gibbs-Duhem correlation they have made temperature corrections, nevertheless, in the Redlich-Kister method.

Delzenne (4), in his study of the binary vapor–liquid equilibrium data, claimed that the validity of his results has been checked by "various criteria"; namely, the van Laar equation and the Redlich-Kister relationship.

It is apparent from these examples that the integrated forms of the Gibbs-Duhem equation and the Redlich-Kister relationship have been considered by these authors as two independent testing methods. The purpose of this note is to point out that these methods are not independent ones.

Redlich and Kister (8) have developed the following relationship:

$$[2] \quad \int_0^1 \log(\gamma_1/\gamma_2)\, dx_1 = 0$$

using Scatchard's excess free energy of mixing in the form of

$$[3] \quad Q = x_1 \log \gamma_1 + x_2 \log \gamma_2$$

and the function

$$[4] \quad dQ/dx_1 = \log(\gamma_1/\gamma_2).$$

Equation [4] may be derived directly from Equation [3] with the condition that the Gibbs-Duhem equation,

$$[5] \quad (\partial \ln \gamma_1/\partial \ln x_1)_{T,P} = (\partial \ln \gamma_2/\partial \ln x_2)_{T,P},$$

be satisfied. A number of integrated forms of Equation [5] are available for correlating activity coefficients (1, 12). It is obvious that the assumptions involved are the same in the Redlich-Kister relationship and in these equations.

The activity coefficients of the integrated forms of Equation [5] are expressed in terms of the liquid mole fraction x. The left-hand side of Equation [2] can be integrated directly with the substitution of these activity coefficients. The integral over the entire composition range is always zero. Some of the examples are illustrated here:

1. Two-suffix Margules equation (12)

$$\log \gamma_1 = x_2^2 A \tag{6a}$$

$$\log \gamma_2 = x_1^2 A \tag{6b}$$

$$\int_0^1 \log \gamma_1 \, dx_1 = \int_0^1 \log \gamma_2 \, dx_1 = A/3$$

$$\therefore \int_0^1 \log(\gamma_1/\gamma_2) \, dx_1 = 0$$

2. Van Laar equation as rearranged by Carlson and Colburn (3)

$$\log \gamma_1 = \frac{A}{(1+Ax_1/Bx_2)^2} \tag{7a}$$

$$\log \gamma_2 = \frac{B}{(1+Bx_2/Ax_1)^2} \tag{7b}$$

$$\int_0^1 \log \gamma_1 \, dx_1 = \int_0^1 \log \gamma_2 \, dx_1 = \frac{A^2B}{(A-B)^3}\left(A - \frac{B^2}{A} + 2B \ln \frac{B}{A}\right)$$

$$\therefore \int_0^1 \log(\gamma_1/\gamma_2) \, dx_1 = 0$$

3. Margules equation as presented by Robinson and Gilliland (9)

$$\ln \gamma_1 = bx_2^2 + cx_2^3 \tag{8a}$$

$$\ln \gamma_2 = bx_1^2 + \tfrac{3}{2} cx_1^2 - cx_1^3 \tag{8b}$$

$$\int_0^1 \ln \gamma_1 \, dx_1 = \int_0^1 \ln \gamma_2 \, dx_1 = \frac{b}{3} - \frac{c}{4}$$

$$\therefore \int_0^1 \log(\gamma_1/\gamma_2) \, dx_1 = 0$$

The same result may be obtained by the substitution of Equation [1] into Equation [2], and from other integrated forms of Equation [5], such as the three-suffix and the four-suffix q-equations of Wohl (12). All these facts indicate that the Redlich-Kister relationship and the integrated forms of the Gibbs-Duhem equation are not independent methods. When the binary vapor–liquid equilibrium data can be represented by one of the integrated

forms of the Gibbs-Duhem equation, there is no need to test the data again using the Redlich-Kister relationship.

When the temperature effect is not negligible in the Gibbs-Duhem correlation, a temperature term may be included in the expression of the activity coefficients, such as the van Laar equation presented by Robinson and Gilliland (9),

$$T \ln \gamma_1 = \frac{B}{[1+A(x_1/x_2)]^2}, \qquad [9a]$$

$$T \ln \gamma_2 = \frac{AB}{(A+x_2/x_1)^2}. \qquad [9b]$$

The corresponding Equation [2] would be

$$\int_0^1 T \log(\gamma_1/\gamma_2)\, dx_1 = 0. \qquad [10]$$

This equation has been suggested recently by Broughton and Brearley (2). From these equations, the same conclusion as presented above may be obtained.

Conclusion:

1. The Redlich-Kister relationship and the integrated forms of the Gibbs-Duhem equation are not independent testing methods of thermodynamic consistency for binary vapor–liquid equilibrium data.

2. When the binary vapor–liquid equilibrium data can be fitted by one of the integrated forms of the Gibbs-Duhem equation, it is not necessary to test the data again using the Redlich-Kister relationship.

3. If the data obey the Redlich-Kister relationship or its modified form, such as Equation [8], they may be expected to be fitted by one of the integrated forms of the Gibbs-Duhem equation.

NOMENCLATURE

A, B, C, D refer to constants used in Equations [1], [6], [7], and [9].
b, c refer to constants used in Equation [8].
P refers to the total pressure.
P^0 refers to the vapor pressure of the pure component.
Q refers to the quantity: Scatchard's excess free energy of mixing/2.303 RT.
R refers to the gas constant.
T refers to the absolute temperature.
x refers to the mole fraction in the liquid.
y refers to the mole fraction in the vapor.
γ refers to activity coefficients, defined as $\gamma_1 = Py_1/P_1{}^0x_1$.
Subscripts 1 and 2 refer to components.

1. Benedict, M., Johnson, C. A., Solomon, E., and Rubin, S. Trans. Am. Inst. Chem. Engrs. 41: 371. 1945.
2. Broughton, D. B. and Brearley, J. M. Ind. Eng. Chem. 47: 838. 1955.
3. Carlson, C. H. and Colburn, A. P. Ind. Eng. Chem. 34: 581. 1942.
4. Delzenne, A. Chem. Eng. Sci. 2: 220. 1952.

5. HANSON, G. H., HOGAN, R. J., RUEHLEN, F. N., and CINES, M. R. Chem. Eng. Progr. Symposium Ser. 49 (6): 37. 1953.
6. HERINGTON, E. F. G. Nature, 160: 610. 1947.
7. OTSUKI, H. and WILLIAMS, F. C. Chem. Eng. Progr. Symposium Ser. 49 (6): 55. 1953.
8. REDLICH, O. and KISTER, A. T. Ind. Eng. Chem. 40: 345. 1948.
9. ROBINSON, C. S. and GILLILAND, E. R. Elements of fractional distillation. 4th ed. McGraw-Hill Book Company, Inc., New York. 1950. pp. 58–59.
10. THIJSSEN, H. S. C. Chem. Eng. Sci. 4: 75. 1955.
11. WALDICHUCK, M., SINGH, R., and SCHMILT, L. W. Paper presented at the 39th Annual Conference of the C. I. C. May, 1956.
12. WOHL, K. Trans. Am. Inst. Chem. Engrs. 42: 215. 1946.

RECEIVED NOVEMBER 9, 1956.
DEPARTMENT OF CHEMICAL ENGINEERING,
UNIVERSITY OF OTTAWA,
OTTAWA, CANADA.

CONTENTS OF VOLUME 34

Adey, A. W. Microwave refractometer cavity design, 519.

Allan, A. B. See King, R. O., 316.

Armstrong, A. M. See Braid, P. E., 45.

Baerg, A. P. See Van Cleave, A. B., 425.

Barncroft, A. R. See Butler, R. M., 340.

Bauer, H. F. A simple apparatus for the change-over from reflux to distillation, 397.

Bourgault, P. L. See Casey, E. J., 95.

Bourgault, P. L., Lake, P. E., Casey, E. J., and **Dubois, A. R.** Nickel–cadmium batteries. II. Impregnation of positive plates by thermal decomposition of aqueous nickel nitrate, 495.

Brady, J. G., Eager, R. L., and **Humphrys, J. M.** An apparatus for differential thermal analysis, 1.

Braid, P. E., Langille, R. C., and **Armstrong, A. M.** Studies in electrostatics: A. Prevention of electrostatic charges on powders. B. Prevention of explosions during hand operations on detonators, 45.

Brown, W. G. and **Colborne, W. G.** Fundamentals of chimney performance, 354.

Brown, W. G. and **Lentz, C. P.** Moisture absorption by some packaging materials at subfreezing temperatures, 366.

Buckholz, E. E. A precision apparatus for applying liquids to test surfaces, 399.

Burr, A. C. and **Neil, D. J.** A thermocouple connection operated by remote control, 88.

Butler, R. M. See Plewes, A. C., 152.

Butler, R. M., Spence, A. E., Barncroft, A. R., and **Plewes, A. C.** The phenol extraction of lubricating oils, 340.

Butler, R. M. and **Tiedje, J. L.** The washing of wax filter cakes, 455.

Casey, E. J. See Bourgault, P. L., 495.

Casey, E. J., Bourgault, P. L., and **Lake, P. E.** Nickel–cadmium batteries. I. Sintered plates from a new Canadian nickel powder, 95.

Cavers, S. D. See Eager, R. L., 121; Gunn, B., 379.

Colborne, W. G. See Brown, W. G., 354.

Craig, B. M. Comparison of the fatty acid composition of rapeseed and mustardseed oils, 335.

Crowe, C. See Misener, A. D., 41.

Cudmore, W. J. G. See Eager, R. L., 121.

Dubois, A. R. See Bourgault, P. L., 495.

Dunne, N. R. See Eager, R. L., 121.

Eager, R. L. See Brady, J. G., 1.

Eager, R. L., Cavers, S. D., Graham, W., Dunne, N. R., and **Cudmore, W. J. G.** Solvent extraction of Saskatchewan lignites. I. Survey of lignites and solvents, 121.

Epstein, N. See Galloway, L. R., 92.

Fraser, R. R. See Pattison, F. L. M., 21.

Furter, W. F. See Johnson, A. I., 413, 429, 514.

Gagnon, P. E., Keirstead, K. F., Walker, J., and **Kavanaugh, K. R.** Hydrolysis of cellulose acetate sulphate in acetone/water solutions, 71.

Gagnon, P. E., Keirstead, K. F., and **Yamasaki, D.** Determination of sulphate acid ester in unstabilized cellulose nitrate, 477.

Galloway, L. R. and **Epstein, N.** A mixture and method for making tough porous uniform spheres, 92.

Giguère, P. A. and **Liu, I. D.** Pressure transducers as recording manometers in chemical kinetics, 473.

Gishler, P. E. See Peterson, W. S., 104.

Goring, D. A. I. The effect of temperature and acidity on the dry storage of sodium carrageenate, 39.
A semimicro gelometer, 53.

Graham, W. See Eager, R. L., 121.

Graham, W. D. Viscosity – weight average molecular weight relationships for dextrans in the higher clinical size range. Reproducibility of the light scattering method, 83.

Guest, R. M. The potentials of zinc and steel in tap water, 245.

Gunn, B., Cavers, S. D., and **Van Cleave, A. B.** The extraction of uranium from a Saskatchewan pegmatite granite, 379.

Hannaford, W. L. W. See Serson, P. H., 232.

Hayes, S. V. See King, R. O., 442.

Huang, C.-J. See Johnson, A. I., 405.

Humphrys, J. M. See Brady, J. G., 1.

Johnson, A. I. and **Furter, W. F.** Salt effect in vapor–liquid equilibrium. Part I, 413. Algebraic representation of vapor–liquid equilibrium data, 429.

Johnson, A. I. and **Huang, C.-J.** Estimation of ideal gas heat capacities of hydrocarbons, 405.

Johnson, A. I., Ward, D. M., and **Furter, W. F.** Vapor–liquid equilibrium data for system: *n*-octane – propionic acid, with salt effect, 514.

Jutras, J. R., Léger, E. G., and **Ouellet, C.** Double enregistrement photoélectrique et manométrique de réactions rapides en phase gazeuse. Application aux flammes froides, 29.

Kavanaugh, K. R. See Gagnon, P. E., 71.

Keirstead, K. F. See Gagnon, P. E., 71, 477.

Keller, H. See Peterson, W. S., 104.

Khalifa, M. Properties of vacuum as a switching ambient, 304.

King, R. O. See Shanfield, H., 10.

King, R. O. and **Allan, A. B.** The oxidation, decomposition, ignition, and detonation of fuel vapors and gases. XXIX. The role of nuclei in the ignition by compression of gaseous heptane–air mixtures: first paper, 316.

King, R. O. and **Hayes, S. V.** The oxidation, decomposition, ignition, and detonation of fuel vapors and gases. XXX. The hydrogen engine and detonation of the end gas by the igniting effect of carbon nuclei formed by pyrolysis of lubricating oil vapor, 442.

Lake, P. E. See Bourgault, P. L., 495; Casey, E. J., 95.

Langille, R. C. See Braid, P. E., 45.

Léger, E. G. See Jutras, J. R., 29.

Lentz, C. P. See Brown, W. G., 366.

Liu, I. D. See Giguère, P. A., 473.

Lu, B. C.-Y. Vapor–liquid equilibrium data for systems methanol–toluene and *n*-propanol–toluene, 468.

A note on thermodynamic consistency tests of binary vapor–liquid equilibrium data, 523.

Lusena, C. V. See Tessier, H., 131.

McIntyre, J. D. and **McMillan, A. F.** An adhesion test for electroplates, 212.

McMillan, A. F. See McIntyre, J. D., 212.

Madonna, L. A. The design and operation of a cloud chamber, 485.

Marris, A. W. Hydraulic stability in the simple surge tank, 182.

Middleton, E. J. See Pattison, F. L. M., 21.

Misener, A. D. and **Crowe, C.** Note on a convenient recording technique for rapid changes, 41.

Mueller, W. A. Corrosion studies of carbon steel in alkaline pulping liquors by the potential–time and polarization curve methods. I. Theory, methods, and selected results, 162.

Neil, D. J. See Burr, A. C., 88.

Niven, C. D. On the friction of heated sleigh runners on ice under high loading, 227. The measurement of the thermal insulation of textiles in wind, 254.

Ouellet, C. See Jutras, J. R., 29.

Pattison, F. L. M., Fraser, R. R., Middleton, E. J., Schneider, J. C., and **Stothers, J. B.** Esters of fluoroacetic acid and 2-fluoroethanol, 21.

Pawliw, J. and **Spinks, J. W. T.** Neutron moisture meter for concrete, 503.

Peterson, W. S., Keller, H., and **Gishler, P. E.** Fluidized solids coking of Canadian heavy crude oils, 104.

Plewes, A. C. See Butler, R. M., 340.

Plewes, A. C., Butler, R. M., and **Pugi, K.** Thermodynamic properties of acetic acid – water, 152.

Pugi, K. See Plewes, A. C., 152.

Rose, D. *With the technical assistance of* **Belec, J. M.** Influence of sugars and glycerol on casein precipitation in frozen milk, 145.
See also Tessier, H., 131, 211.

Rose, D. and **Tessier, H.** Effect of heat and of prefreezing storage on the stability of frozen milk, 139.

Roxburgh, J. M. The explosive characteristics of elevator dusts, 260.

Roxburgh, J. M., Spencer, J. F. T., and **Sallans, H. R.** Recovery of polyhydric alcohols from yeast fermentations, 248.
Description of 5-liter stainless steel fermentors, 389.

Sallans, H. R. See Roxburgh, J. M., 248, 389.

Satyanarayana, B. S. A note on the measurement of Vickers hardness indentations, 375.

Schneider, J. C. See Pattison, F. L. M., 21.

Serson, P. H. and **Hannaford, W. L. W.** A portable electrical magnetometer, 232.

Shanfield, H. and **King, R. O.** The decomposition, oxidation, ignition, and detonation of fuel vapors and gases. XXVIII. The thermal decomposition of *n*-pentane as affected by the flow configuration in King reactor No. 10, 10.

Smith, D. S. Electrodeless discharge lamp exciter, 521.

Spence, A. E. See Butler, R. M., 340.

Spencer, J. F. T. See Roxburgh, J. M., 248, 389.

Spinks, J. W. T. See Pawliw, J., 503.

Steiner, G. and **Tarr, H. L. A.** Penetration of chlortetracycline into fish muscle and its destruction by heat, 215.

Stothers, J. B. See Pattison, F. L. M., 21.

Tarr, H. L. A. See Steiner, G., 215.

Tessier, H. See Rose, D., 139.

Tessier, H. and **Rose, D.** Composition of the liquid portion of frozen milk, 211.

Tessier, H., Rose, D., and **Lusena, C. V.** Lactose crystallization in frozen milk, 131.

Tiedje, J. L. See Butler, R. M., 455.

Van Cleave, A. B. See Gunn, B., 379.

Van Cleave, A. B. and **Baerg, A. P.** The extraction of Th^{230} (ionium) from a Canadian pitchblende residue, 425.

Vincent, D. L. The preparation of sodium alginate from rockweed, 220.

Wait, J. R. On the measurement of the conductivity of a fluid contained in a cylindrical vessel, 410.

Wait, J. R. and **Walpole, R. E.** Calculated radiation characteristics of slots cut in metal sheets. II, 60.

Walker, J. See Gagnon, P. E., 71.

Walpole, R. E. See Wait, J. R., 60.

Ward, D. M. See Johnson, A. I., 514.

Watson, J. S. An all glass circulating pump for gases, 373.

Whalley, E. The design of pressure vessels subjected to thermal stress. I. General theory for monoblock vessels, 268.
The design of pressure vessels subjected to thermal stress. II. Steady state temperature distribution, 291.

Wright, G. F. A useful modification of the Hershberg melting point apparatus, 89.

Yamasaki, D. See Gagnon, P. E., 477.

ANNOUNCEMENT

This is to announce that Volume 34 of the Canadian Journal of Technology will include two additional numbers (Nos. 7 and 8) to be published in January and March, 1957. Volume 35 of the Canadian Journal of Technology will then be published (under a new name, to be announced) under the auspices of the Chemical Institute of Canada.